

Food & Function

Linking the chemistry and physics of food with health and nutrition

Accepted Manuscript

This article can be cited before page numbers have been issued, to do this please use: J. I. Mosele, B. Viadel, S. Yuste, L. Tomás, S. García, M. T. Escribano-Bailon, I. García-Estévez, P. Moretón, F. Rodríguez de Rivera, S. de Domingo and M. J. Motilva, *Food Funct.*, 2024, DOI: 10.1039/D4FO03774J.



This is an Accepted Manuscript, which has been through the Royal Society of Chemistry peer review process and has been accepted for publication.

Accepted Manuscripts are published online shortly after acceptance, before technical editing, formatting and proof reading. Using this free service, authors can make their results available to the community, in citable form, before we publish the edited article. We will replace this Accepted Manuscript with the edited and formatted Advance Article as soon as it is available.

You can find more information about Accepted Manuscripts in the [Information for Authors](#).

Please note that technical editing may introduce minor changes to the text and/or graphics, which may alter content. The journal's standard [Terms & Conditions](#) and the [Ethical guidelines](#) still apply. In no event shall the Royal Society of Chemistry be held responsible for any errors or omissions in this Accepted Manuscript or any consequences arising from the use of any information it contains.

1 **Application of dynamic colonic gastrointestinal digestion model to red wines: study**
2 **of flavanol metabolism by gut microbiota and cardioprotective activity of**
3 **microbial metabolites**

4
5 Juana I. Mosele^{1,2}, Blanca Viadel³, Silvia Yuste^{1,4}, Lidia Tomás-Cobos³, Sandra
6 García³, María-Teresa Escribano Bailón⁵, Ignacio García Estévez⁵, Pilar Moretón
7 Fraile⁴, Fernando Rodríguez de Rivera⁴, Soledad de Domingo Casado⁴, María-José
8 Motilva¹

9
10 ¹Instituto de Ciencias de la Vid y del Vino-ICVV (Consejo Superior de Investigaciones
11 Científicas-CSIC, Universidad de La Rioja-UR, Gobierno de La Rioja), Finca La
12 Grajera, Ctra. de Burgos Km. 6 (LO-20, - salida 13), 26007 Logroño, Spain.

13 ²Fisicoquímica, Facultad de Farmacia y Bioquímica-IBIMOL, Universidad de Buenos
14 Aries-CONICET, 1113 Buenos Aires, Argentina.

15 ³Ainia, Technology Centre, C/Benjamin Franklin 5-11, 46980 Paterna (Valencia), Spain.

16 ⁴Antioxidants Research Group, Food Technology Department, Agrotecnio-RECERCA
17 Center, University of Lleida, 25198 Lleida, Spain.

18 ⁵Department of Analytical Chemistry, Nutrition and Food Science, Universidad de
19 Salamanca, Campus Miguel de Unamuno s/n, E37007, Salamanca, Spain.

20 ⁶Bodegas Pradorey, Real Sitio de Ventosilla SA, Gumiel de Mercado, Burgos, Spain

21
22 ***Corresponding author:** E-mail: motilva@icvv.es
23



24 **Abstract**View Article Online
DOI: 10.1039/D4FO03774J

25 Over the last decade, research has emphasized the role of the microbiome in regulating
26 cardiovascular physiology and disease progression. Understanding the interplay between
27 wine polyphenols, gut microbiota, and cardiovascular health could provide valuable
28 insights for uncovering novel therapeutic strategies aimed at preventing and managing
29 cardiovascular disease. In this study, two commercial red wines were submitted to an *in-*
30 *vitro* dynamic gastrointestinal digestion (GIS) to monitor the flavanol-microbiota
31 interaction by evaluating the resulting microbial metabolites. Furthermore, the
32 cardiovascular protective activity of wine flavanol microbial metabolites was
33 investigated, integrating their effects on antihypertensive activity, cholesterol metabolism
34 and insulin resistance into human endothelial (HAECs) and hepatic (HepG2) cell lines.
35 A significant production of microbial flavanol metabolites, with a prevalence of
36 phenylpropionic and phenylacetic acids, valerolactones and short chain fatty acids like
37 butyric acid was observed, particularly in the transverse and descending colon sections.
38 Incubating HAECs and HepG2 cells with the colon improved cardioprotective
39 parameters. Specifically, an increase in the vasodilator NO, an improvement in the LDL
40 receptors and the HMGCoA enzyme, with positive effects on cholesterol metabolism, and
41 the reduction of the glycogen levels improving the insulin resistance were observed.

42 **Keywords:** cardioprotection, colonic metabolism, dynamic digestion model, flavanols,
43 microbial metabolism, red wine, UHPLC-QqQ-MS/MS.

44



45 1. Introduction

46 Wine differs from other alcoholic beverages due to its heterogeneous (poly)phenol
47 content, among which flavanols are prominent components¹. In wine, flavanols are
48 present as monomers (catechin, epicatechin and epigallocatechin) as well as
49 proanthocyanidin oligomers or polymers exhibiting varying degrees of polymerization
50 according to the structural monomeric units¹. Beyond imparting sensory and preservative
51 attributes^{2,3}, moderate consumption of wine containing flavanols has been associated with
52 the prevention of cardiovascular disease (CVD)⁴.

53 (Poly)phenol bioactivity hinges on their bioavailability. While monomers of flavanols
54 are partially absorbed in the small intestine during gastrointestinal digestion intact
55 proanthocyanidins do not undergo absorption⁵. After gastrointestinal absorption,
56 subsequent biomodifications of flavanol monomers occur, particularly in the liver,
57 yielding diverse sulphated, glucuronidated, and methylated phase-II conjugated
58 metabolites^{5,6}. Some conjugated metabolites re-enter the enterohepatic recirculation,
59 reaching the colon together with the non-absorbed flavanols. Within the gut, microbial
60 action catalyzes transformations as dehydroxylation, demethylation, ring fission and
61 decarboxylation generating low molecular weight compounds, such as phenolic acids,
62 phenyl-valerolactones and phenyl-valeric acids^{5,7}. These colonic catabolites can be
63 absorbed by colonocytes, increasing the overall bioavailability of flavanols and
64 diversifying the spectrum of bioactive molecules^{5,7,8}. The flavanol catabolites generated
65 by the gut microbiota may exert more biological effect than their parent compounds⁹.
66 Moreover, the interactions between flavanols and gut microbiota are intricate and
67 reciprocal, influencing microbiome richness, diversity, composition and function^{10,11}.
68 Understanding the colonic metabolism and flavanol-gut microbiota interactions is pivotal



69 for unraveling wine-health relationships and identifying molecules potentially involved
70 in CVD prevention.

71 Therefore, to explore and determine the mechanisms of action of (poly)phenols and
72 their role in disease prevention, it is crucial to understand the factors that constrain their
73 bioactivity. Dynamic *in-vitro* models simulating human digestion serve as simple and
74 ethical alternatives for assessing the digestibility, stability, structural changes and bio-
75 accessibility of food bioactive compounds. The multi-compartmental Gastro-Intestinal
76 Simulator (GIS) systems comprising (i) gastric (ii) duodenal and (iii) a jejunal chambers,
77 coupled with a system of trichamber colonic fermentation including (iv) ascending (AC),
78 (v) transversal (TC) and (vi) descending colon (DC) inoculated with human feces or gut
79 microbiota. Different studies have applied these dynamic digestion *in-vitro* models
80 mimicking the human gut environment to study the two-way interaction between the gut
81 microbiota and phenolic compounds that is pivotal in determining their beneficial effects
82 in human health^{12,13}.

83 Many studies on (poly)phenols to date have focused on the bioactivities of one specific
84 molecule in aglycone form, often at supraphysiological doses, whereas foods contain
85 complex mixtures with multiple additive or interfering activities¹⁴. In the specific case of
86 wine flavanols, most of the bioactivity studies in cell line models have been carried out
87 with the monomers catechin and epicatechin, omitting the complex mixture of
88 proanthocyanidins that during the gastrointestinal digestion are hydrolysed into
89 monomers which are subsequently strongly metabolized by gut microbiota. Therefore,
90 the main objective of this study was to deepen the understanding of the potential
91 cardioprotective effects of colonic metabolites derived from wine flavanols. For this, two
92 commercial Tempranillo red wines (2020 and 2021 harvest) were selected based on their
93 high flavanol contents. The wines were submitted to an *in-vitro* dynamic GIS to monitor

View Article Online
DOI: 10.1039/D4FO03774J



94 the stability and transformation of flavanols during the gastro-intestinal digestion and to
95 determine the main microbial metabolites produced after their colonic fermentation.
96 Furthermore, the cardiovascular protective activity of wine flavanol microbial
97 metabolites was investigated, integrating their effects on antihypertensive activity,
98 cholesterol metabolism, and insulin resistance in human endothelial (HAECs) and hepatic
99 (HepG2) cell lines.

100 **2. Materials and Methods**

101 **2.1. Wine samples and determination of flavanol content**

102 Red wines from both the 2020 and 2021 harvests were elaborated from *Vitis vinifera*
103 L. cv. Tempranillo grapes by Bodegas Pradorey (Burgos, Spain). Alcoholic fermentation
104 was performed in stainless steel tanks and malolactic fermentation and ageing was carried
105 out in French oak barrels for 1 year before bottling. Prior to conducting the HPLC-DAD-
106 ESI-MS analysis of flavanols, wines were fractionated using a cationic exchange
107 cartridge (Oasis MCX, Waters Corp., Milford, MA, USA) as previously reported¹²¹⁵.
108 Chlorogenic acid (Sigma-Aldrich, St. Louis, MO, USA) was incorporated into the
109 samples as an internal standard, achieving a final concentration of 0.025 mg/mL. Then,
110 chromatographic separation was achieved using an Agilent 1200 series HPLC system
111 equipped with an Agilent Poroshell 120 EC-18 column (2.7 μm , 4.6 mm \times 150 mm)
112 (Agilent Technologies, Waldbronn, Germany), maintained at a temperature of 25° C. The
113 mobile phase was composed by solvent A, 0.1% (v/v) formic acid (VWR International,
114 Fontenay-sous Bois, France) aqueous solution, and solvent B, HPLC grade acetonitrile
115 (Merck KGaA, Darmstadt, Germany). Flavanols were quantified through mass
116 spectrometry using a 3200 QTRAP triple quadrupole mass spectrometer (AB Sciex,
117 USA) equipped with an electrospray ionization source (ESI Turbo V™ Source). The
118 detailed conditions for the HPLC and mass spectrometry procedures are provided by



119 García-Estévez et al. (2017)¹⁵. Calibration curves for (+)-catechin, (-)-epicatechin,
 120 procyanidin dimers B1 and B2, procyanidin trimer C1, (-)-epicatechin 3-*O*-gallate, (+)-
 121 gallo catechin, and (-)-epigallocatechin were utilized for quantification. Monomeric
 122 flavanols were purchased from Sigma-Aldrich (St. Louis, MO, USA), whereas
 123 procyanidin dimers and trimer were purchased from Extrasynthèse (Genay, France).
 124 When the corresponding standard was not available, the flavanol was quantified as
 125 equivalents of the most related flavanol on the basis of their structure. Thus, procyanidin
 126 dimers B3 and B7 were quantified as procyanidin dimer B1 equivalents; procyanidin
 127 dimers B4, B5, B6 and B7 were quantified as procyanidin dimer B2 equivalents,
 128 procyanidin trimers, tetramers and pentamers were quantified as procyanidin trimer C1
 129 equivalents and prodelfinidins were quantified as gallo catechin equivalents. The
 130 flavanol composition of red wines from the 2020 and 2021 harvests is detailed in Table
 131 1. The wine flavanol concentration was expressed as mean \pm standard deviation (SD) of
 132 the average of 3 replicates per wine.

133 **Table 1.** Flavanol concentration in red wines from the 2020 and 2021 harvests.
 134
 135

Compound (mg/L wine)	Wine 2020	Wine 2021
Catechin	5.0 \pm 0.3	4.7 \pm 0.2
Epicatechin	6 \pm 1	13.4 \pm 0.3
Galocatechin	1.57 \pm 0.09	1.62 \pm 0.01
Epigallocatechin	1.01 \pm 0.02	1.4 \pm 0.1
Epigallocatechin gallate	0.003 \pm 2E-05	0.002 \pm 2E-05
Epicatechin gallate	0.010 \pm 0.001	0.11 \pm 0.01
<i>Total flavan-3-ols monomers</i>	13.6 \pm 1	21.2 \pm 0.6
Procyanidin dimer B1	42.3 \pm 0.4	29.9 \pm 0.4
Procyanidin dimer B2	19.5 \pm 0.6	16.8 \pm 0.6
Procyanidin dimer B3	3.3 \pm 0.1	4.3 \pm 0.1
<i>Total proanthocyanidins dimers</i>	82 \pm 2	82 \pm 2
<i>Total proanthocyanidins trimers</i>	7.6 \pm 0.9	9.0 \pm 0.5
<i>Total proanthocyanidins tetramers</i>	3.9 \pm 0.2	5.6 \pm 0.1
<i>Total proanthocyanidins pentamers</i>	0.36 \pm 0.01	0.54 \pm 0.01
<i>Total gallo catechins and prodelfinidins</i>	6.4 \pm 0.3	7.3 \pm 0.3
<i>Total catechins and procyanidins</i>	105 \pm 7	114 \pm 2



Total flavanols	111 ± 8	122 ± 2
Results are expressed as mean ± standard deviation (SD)(n=3)		

View Article Online

DOI: 10.1039/D4FO03774J

136
137

138 2.2. Simulated digestion in the Dynamic Colonic Gastrointestinal Digester

139 The Dynamic-Colonic Gastrointestinal Digester (D-CGD) was developed by AINIA
 140 Technology Center (Valencia, Spain)¹⁶. The system consists of a computer-assisted
 141 model of five interconnected double jacket vessels imitating the physiological conditions
 142 of the stomach (G: vessel 1), small intestine (I: vessel 2), and the three colonic sections:
 143 the AC (vessel 3), the TC (vessel 4), and the DC (vessel 5) (Supplemental Figure S1). All
 144 the compartments were connected by peristaltic pumps, working semi-continuously in G
 145 and I and continuously in AC, TC and DC. The system set up, that is, the volumetric
 146 capacity, pH, anaerobiosis (O₂ and CO₂ levels), and temperature (37 °C) were
 147 controlled¹⁶. The pH was continuously controlled in the compartments for the stomach
 148 (following pH changes during gastric digestion, from pH 4,8 to pH 1,7) and the small
 149 intestine (pH 6.5–7), using secretions of 1 mol/L hydrochloric acid and 1 mol/L sodium
 150 bicarbonate, respectively¹⁷. Anaerobiosis of the system was achieved by the addition of
 151 nitrogen¹⁶.

152 2.2.1. Dynamic gastrointestinal digestion

153 The dynamic gastrointestinal digestion consisted of two steps, a gastric digestion (G)
 154 (2 h) followed by an intestinal digestion (I) (6 h)¹⁶. Digestion in G was performed by
 155 adding a continuous flow of 0.03 % (w/v) pepsin (from porcine mucosa, ≥ 2500 unit/g;
 156 P7012–56, Sigma-Aldrich, Spain) to a gastric electrolytic solution. The gastric pH
 157 medium was set up according to a pH curve observed in *in-vivo* data by adding a HCl
 158 solution (1 M) (HCl, 37 % purity, VWR Chemicals, Spain). After 2 h, the gastric digested
 159 material generated was immediately transferred to I vessel, where simulated digestion
 160 was conducted via the continuous addition of an intestinal solution consisting of
 161 pancreatin (1.9 g/L) (pancreatin P1750–100 G, Sigma-Aldrich, Spain), NaHCO₃ (12 g/L)



162 (Merck, Germany), and Oxgall dehydrated fresh bile (6 g/L, bile bovine, B3883, BD
163 USA) in distilled water (240 mL for the whole intestinal digestion step). After that, the
164 intestinal digested material generated was immediately transferred to the third vessel
165 (AC) for 30 min, simulating the digestion transfer through the ileocecal valve to the AC.
166 The transferred material was maintained in the whole colonic segment for 76 h under a
167 continuous dynamic flow from the AC entrance to the DC exit, according to Rosès et al.
168 (2023)¹⁸.

169 2.2.2. *Dynamic in-vitro colonic fermentation*

170 Fresh feces from 4 healthy adults, non-smokers, with no history of antibiotic use in the
171 previous three months and no background of intestinal disease were collected and
172 transported in special anaerobic bags (BDGasPak™ systems) (Becton, Dickinson and
173 Company, NJ, USA). The samples were diluted and regenerated in a physiological
174 phosphate buffer with thioglycolate 20 % (w/v) (Merk, Spain). This mixture was then
175 homogenized in a stomacher and centrifuged at 3000g for 15 min (Heraeus Multifuge
176 x3R Centrifuga, Thermo Scientific, Spain). The supernatant was collected and inoculated
177 in the colon vessels (Supplemental Figure S1) according to Roses et al. (2021)¹⁹. Hence,
178 50, 80 and 60 mL of the collected supernatant were placed in the AC section, the TC
179 section, and the DC section, respectively, and filled with culture medium²⁰ up to a total
180 volume of 1000, 1600 and 1200 mL, respectively, allowing simulation of the conditions
181 of the human colon media.

182 2.2.3. *Experimental protocol: in-vitro gastrointestinal digestion and colonic fermentation* 183 *of red wine*

184 The experimental design and set-up are depicted in Figure 1. The experiment was
185 composed of two different phases. First, a stabilization period of 12 days (days 0 to 12),
186 where a stable colonic microbiota was reached, followed by a wine treatment period of



187 14 days (days 13 to 26), where the microbiota was fed with red wine once per day. For
188 the microbiota stabilization period (day 0 to day 12), 200 mL of culture medium were
189 added to G three times a day. After the stabilization period, and during the wine treatment
190 period (days 13 to 26), the system was fed with 100 mL of red wine once a day (up to a
191 final volume of 200 mL) and with 200 mL of cultured medium twice a day^{20,21}. Samples
192 of culture medium from the three colonic reactors (AC, TC, DC) were collected at
193 different times during the stabilization (days 0, 5, 7 and 12) and treatment (days 13-16,
194 18-21, 23 and 26) periods and used for further analysis (Figure 1).

195 **2.3. Analysis of wine flavanols and their microbial metabolites by ultra-high** 196 **performance liquid chromatography with triple-quadrupole mass spectrometry** 197 **(UHPLC/QqQ-MS/MS) in different digestion steps**

198 The monitored of wine flavanol transformation during the continuous gastrointestinal
199 digestion and colonic fermentation was conducted through UHPLC-QqQ-MS/MS.
200 Samples (50 mL media) were collected from each section (Figure 1) at the end of the
201 stabilization period (day 12) and during the treatment period (days 13, 14, 15, 16, 18, 20,
202 23 and 26) and stored at -80° C until analysis. Prior to the chromatographic analysis, the
203 samples were filtered (PTFE syringe filters, 0.22 µm pore size, Scharlab Chemie,
204 Sentmenat, Catalonia, Spain) and analyzed by UHPLC-QqQ-MS/MS based on the
205 method described by Royo et al. (2021)²². Separation of analytes was carried out in a
206 liquid chromatograph (Shimadzu Nexera, Shimadzu Corporation, Japan), coupled to a
207 3200QTRAP triple quadrupole mass spectrometer (AB Sciex, USA) equipped with an
208 electrospray ionization source (ESI Turbo V™ Source). The (poly)phenol separation was
209 performed in a Waters AcQuity BEH C18 column (100 mm × 2.1 mm, 1.7 µm) equipped
210 with a VanGuard™ AcQuity BEH C18 pre-column (5 × 2.1 mm, 1.7 µm) (Milford, MA,



211 USA). The electrospray (ESI) interface was used in the negative mode [M-H]⁻. Data
212 acquisition was carried out with the Analyst® 1.6.2 software (AB Sciex, USA).

213 The wine flavanol metabolites were identified by comparing their spectra and retention
214 times with those of externally injected standards. Compounds for which standards were
215 not available were tentatively identified using MRM transitions with the mass of the
216 parent ion (M-H) and typical MS fragmentation pattern described in the literature. Some
217 of the compounds were quantified using the calibration curves of their corresponding
218 commercial standards. The other compounds were tentatively quantified using the
219 calibration curves of standards with similar chemical structures. Supplementary Table S1
220 shows the selected reaction monitoring (SRM) conditions, the cone voltage and collision
221 energy and the commercial standard used for quantification. The concentration of the
222 wine flavanols and their microbial metabolites in the gastrointestinal and colon media
223 (AC, TC and DC) was expressed as mean of the average of two replicates.

224 The phenol commercial standards used for the identification and quantification were
225 epicatechin and procyanidin B2 (Extrasynthese), procyanidin B1 (Purifa, Dongguan,
226 China), catechin, 4-hydroxybenzoic acid, 4-hydroxyphenylacetic acid, 3,4-
227 dihydroxybenzoic acid (protocatechuic acid), *trans*-coumaric acid, gallic acid and 4,4-
228 bis(4-hydroxyphenyl)valeric acid (Sigma-Aldrich), 5-(3',4'-dihydroxyphenyl)- δ -
229 valerolactone (TransMIT, Gießen, Germany), 3-(3,4-dihydroxyphenyl)propionic acid
230 and 3,4-dihydroxyphenylacetic acid (Alfa Aesar, Massachusetts, USA), 3-(3-
231 hydroxyphenyl)propionic acid (Biosynth Carbosynth, Compton, United Kingdom),
232 hippuric acid and 3-phenylpropionic acid (Thermo Fisher Scientific, Waltham, MA,
233 USA), catechol (TCI, Tokio, Japan), pyrogallol (Glentham Life Sciences, Corsham,
234 United Kingdom) and galocatechin (Target Mol, Massachusetts, USA). Stock solutions
235 of the standard were prepared in methanol (1000 mg/L) and stored at -20° C. Methanol



236 (HPLC grade), formic acid (HPLC grade), acetonitrile (HPLC grade) and HCl were
237 purchased from VWR Chemicals BDH Prolabo (Leuven, Belgium). The water was Milli-
238 Q quality (Millipore Corp, Bedford, MA, USA).

239 **2.4. Microbiota analysis**

240 The microbial population during the stabilization and wine treatment periods was
241 checked by bacteria plate counts. Culture medium samples were collected by duplicate at
242 different days (days 0, 5, 7, 12) of the stabilization period to monitor the maintenance of
243 microbial populations and at different days during the wine treatment period (days 14,
244 19, 21 and 26) (Figure 1). Ten milliliters of media were taken from each colon reactor
245 and serially diluted in saline solution. The plates were inoculated with 1 mL of 4 serial
246 dilutions of the media by duplicate and incubated at 37° C under aerobic or anaerobic
247 conditions. The following bacterial groups were quantified by the direct plating method
248 on specific colonic culture medium (CFU/mL): *Lactobacillus* (MRS agar using the
249 MALDI-TOF technique to verify lactobacilli colonies), *Bifidobacterium* (TOS-
250 propionate agar enriched with MUP), *Enterobacter* (VRBD agar), *Clostridium* (TSC agar
251 enriched with cycloserin) and total anaerobic bacteria (Schaedler agar). Results were
252 expressed as Log CFU/mL culture medium.

253 **2.5. Determination of short-chain fatty acids (SCFA)**

254 Culture medium samples were collected in triplicate from each reactor (AC, TC and
255 DC) at the end of the stabilization (day 12) and wine treatment (day 26) periods (Figure
256 1). Samples were pooled and filtered (0.2 µm filters) previously to chromatographic
257 analysis. The microbial SCFA acetic, propionic and butyric acids were analyzed by gas
258 chromatography coupled with a flame-ionization detector (GC-FID) after liquid-liquid
259 extraction. Briefly, ethyl acetate containing capric acid as the internal standard (IS) were
260 added to 10 mL of medium sample collected from each reactor (AC, TC and DC), mixed



261 during 10 min and centrifuged. The supernatant was filtered and injected into a GC-FID
262 (AS 800 C.U., CE Instruments, Wigan, United Kingdom) equipped with an HP-FFAP 25
263 m x 0.2 mm x 0.33 mm column (Agilent Technologies, Santa Clara, CA, USA). The
264 SCFA were quantified by interpolation in the calibration curve using capric acid as IS.

265 **2.6. Cell culture assays**

266 *2.6.1. Cell cultures*

267 Endothelial (EA.hy926) and human hepatic (Hep G2) cell lines (both from the
268 American Type Culture Collection, Manassas, VA, USA) were used as vascular
269 homeostasis, and cholesterol and insulin resistance models, respectively, to conduct the
270 functional analysis of wine flavanol colonic metabolites. The cells were cultured in high
271 glucose-DMEM (Sigma-Aldrich, St. Louis, MO, USA) supplemented with 10% of fetal
272 bovine serum (Gibco, BRL, Australia) and 1 % penicillin-streptomycin at 37° C in a
273 humidified atmosphere of 5% CO₂. The medium was changed every 2-3 days until it
274 reached a 90% confluence.

275 *2.6.2. Preparation of the test samples*

276 Medium culture samples from DC reactor at the end of the stabilization (day 12) and
277 wine treatment (day 26) periods (Figure 1) respectively, were collected in triplicate,
278 pooled, and filtered (0.2 µm filters). Each sample was measured, adjusted to 6-8 pH and
279 stored at -20° C until the subsequent experiments.

280 *2.6.3. Cell viability assay*

281 To define the non-toxic levels of microbial wine flavanol metabolites present in the
282 culture medium samples from DC colon reactor, cell viability was evaluated through a
283 fluori-colorimetric assay. Briefly, 2×10^4 cells were seeded in 96-well plates and treated
284 with different serial dilutions from the samples of the DC (days 12 and 26) at 37° C and
285 5 % CO₂-humidity environmental. After 24 h of treatment, the cell media was replaced



286 with 10 % Alamar Blue reagent (Invitrogen, Waltham, MA, USA) in PBS for 2 h and
287 colorimetry was measured using a spectrofluorometer (Fluoroskan, Thermo Fisher
288 Scientific, Waltham, MA, USA) at λ excitation = 540 nm and λ emission = 590 nm.

289 Considering the straight relation between fluorescence and cellular viability, the equation
290 was as follows:

291 % Viability = (Fluorescence units in the sample / Fluorescence units in the control) x 100

292 2.6.4. Cell treatments

293 2.6.4.1. NO and END-1 production

294 EA.hy926 cells were seeded in 24-well plates at $1 \cdot 10^5$ cells/well. The following day,
295 the PBS was depleted from the media and the cells were cultured for 24 h at 37 °C. The
296 cells were then treated for 2 h with a 1/8 dilution of the culture medium samples obtained
297 from DC colon reactor at day 12 (control media) and at day 26 corresponding to the end
298 of the wine treatment period (media contained microbial wine flavanols) (Figure 1). After
299 DC media treatment, the IL-1b (100 ng/mL) was added and remained overnight. After 24
300 h, the cell supernatant was collected, and the NO was measured using Griess reagent
301 (Merck, Darmstadt, Germany) and following the manufacturer's protocol. Additionally,
302 the EA.hy926 cells were collected for RNA extraction and measurement of the END-1
303 gene expression.

304 2.6.4.2. Cholesterol metabolism

305 HepG2 cells were seeded in 12-well plates at $2.5 \cdot 10^5$ cells/well. After 24 h, the cells
306 were treated with the DC culture medium samples (days 12 and 26) (Figure 1) described
307 above and incubated for 24 h at 37 °C. After the incubation period, the cells were collected
308 for measurement of LDLr and HMGCo-R gene expression (Thermo Fisher Scientific).

309 2.6.4.3. Insulin resistance



310 To determine the hepatocyte glycogen storage, Hep2 cells were seeded in 12-well
311 plates at $2.5 \cdot 10^5$ cells/well. The cells were incubated with 100 mM of insulin for 24 h at
312 37 °C and then the hepatocytes were treated with the DC media samples (days 12 and 26)
313 (Figure 1) described above for another 24 h. After this period, cells were washed three
314 times with PBS and collected for determination of glycogen. The glycogen content in the
315 cells was assayed by using anthrone reagent (Sigma-Aldrich), and the amount of blue
316 compound generated by this reaction was detected on the 620 nm wavelength using a
317 microplate reader (Thermo Fisher Scientific). In addition, the protein content of the
318 collected HepG2 cells was quantified by the BCA method (Thermo Fisher Scientific),
319 and the values were shown as the ratio of glycogen (mg)/protein (mg). Another 12-well
320 plate with the same treatment was collected for measurement of the Akt gene expression
321 (Thermo Fisher Scientific).

322 2.6.5. Real time quantitative RT-PCR

323 For determination of the gene expression, RNA extraction from different experiments
324 was carried out automatically with the MAXWELL equipment (Promega Corporation,
325 Madison, WI, USA). cDNA was obtained from RNA using the High-Capacity cDNA
326 reverse transcription kit (Applied Biosystems, Foster City, CA, USA). To study the
327 cholesterol metabolism, real-time PCR was performed using the END-1, HMGCo-R,
328 LDLr and Akt primers (Thermo-Fisher Scientific) as biomarkers.

329 The glyceraldehyde-3-phosphate dehydrogenase (GAPDH) gene (Thermo-Fisher
330 Scientific) was used as a housekeeping gene, whose expression is constitutive in these
331 cells. The amplification conditions in the thermocycler 7300 (Applied Biosystems, CA,
332 USA) were universal and the quantification of gene expression was performed in a
333 relative way, so that the magnitude of the physiological changes in the biomarker gene



334 was obtained in comparison with the housekeeping gene. For calculations, the formula $2^{-\Delta\Delta Ct}$ was used.

336 2.7. Statistical analysis

337 Microbiota count and SCFA concentration, respectively, in culture medium were
338 expressed as mean \pm standard deviation (SD) of the average of two replicates. Cell line
339 results were expressed as mean \pm SD of the average of two independent studies, including
340 2 replicates per study (n=4). One-way analysis of variance (ANOVA), using Fisher's least
341 significant difference (LSD) test, was used to determine significant differences ($p < 0.05$)
342 between data from cells incubated with culture medium before and after wine treatment.
343 All the statistical analyses were carried out using GraphPad Prism 9 version 9.4.1 for
344 Windows (GraphPad Software, San Diego, California USA).

345 3. Results and discussion

346 The bioactivity of red wines has been associated with the presence of flavanols. In this
347 work, two different red wines from two consecutive seasons (2020 and 2021), were
348 submitted to a dynamic gastrointestinal digestion model, including colonic fermentation,
349 to study the potential cardioprotective and insulin resistance effects of flavanol colonic
350 metabolites.

351 3.1. Stability and kinetic of wine flavanols during the dynamic *in-vitro* 352 gastrointestinal digestion

353 Absorption of dietary components occurs predominantly during gastrointestinal
354 digestion. With only limited exceptions, the bioavailability of food phenolic compounds
355 is low, particularly in the case of the oligomeric and polymeric forms of flavanols, like
356 proanthocyanidins⁵. Consequently, the beneficial effects attributed to the flavanol
357 fraction of wine appear to be primarily linked with the non-absorbed compounds that



358 transit to the colon. To evaluate the stability of phenolic compounds during
359 gastrointestinal digestion and, therefore, predict the amount and nature of flavanols
360 reaching the colon, we performed simulated gastric and intestinal digestion. Interestingly,
361 the digestion of the selected red wines from the two consecutive harvests (2020 and 2021)
362 showed a similar trend (Table 2 and Supplemental Tables S2 and S5), which validates the
363 results. In line with the data published by Tamargo et al. (2023)²³, we also observed a
364 gradual decrease in the wine flavanol (precursors) concentration in the media throughout
365 the dynamic *in-vitro* gastrointestinal digestion, with partial and complete disappearance
366 after the gastric and intestinal phases, respectively (Table 2). Regarding the phenolic
367 acids, the concentration of *p*-coumaric acid in the media increased after the intestinal
368 digestion phase (Table 2). The concentration of protocatechuic acid was similar to that
369 detected in the digestion media plus wine, before digestion. While gallic acid remained
370 largely unaffected after the gastric step, it was not detected after the intestinal digestion
371 phase. The increase in the concentration of the *p*-coumaric acids after intestinal digestion,
372 could be related to the release on the polyphenols covalently bound to wine proteins²⁴.

View Article Online
DOI: 10.1039/D4FO03774J



373 **Table 2.** Phenolic composition of the media after the gastric and intestinal digestion of the 2020 and 2021 wines, respectively. Var: percentage of
 374 variation in the phenol concentration after the gastric and intestinal digestion in relation to media+wine.
 375

Phenolic compound	2020 wine (mg/L wine)					2021 wine (mg/L wine)				
	Media+wine	Gastric digestion	Var (%)	Intestinal digestion	Var (%)	Media+wine	Gastric digestion	Var (%)	Intestinal digestion	Var (%)
<i>p</i> -coumaric acids	0.50	0.40	-20	1.52	204	1.04	0.91	-12	2.18	110
Protocatechuic acid	1.26	1.15	-9	0.96	-24	1.02	0.90	-12	1.00	-2
Gallic acid	10.1	9.38	-7	nd	-100	14.0	13.3	-4	0.19	-99
Catechin	4.18	3.02	-28	nd	-100	5.92	3.34	-44	0.32	-95
Epicatechin	2.13	1.50	-30	nd	-100	2.51	1.35	-46	0.09	-96
Gallocatechin	0.74	0.52	-30	nd	-100	1.30	0.78	-40	nd	-100
Epigallocatechin	0.80	0.54	-33	nd	-100	0.72	0.40	-45	nd	-100
Epigallocatechin gallate						0.04	0.07	96	nd	-100
Procyanidin B1	7.72	4.62	-40	nd	-100	9.80	4.10	-58	0.46	-95
Procyanidin B2	1.89	1.20	-37	nd	-100	2.43	1.21	-50	nd	-100
Procyanidin B3	0.52	0.42	-19	nd	-100	0.55	0.29	-47	nd	-100
Procyanidin T	0.02	0.01	-50	nd	-100	0.08	0.06	-28	nd	-100

376 Results are expressed as mean (n=2). nd: not detected.

377



378 **3.2. Flavanol kinetic metabolism in different colon segments during the dynamic**
379 **colonic fermentation of wine**

380 The kinetic of the wine flavanol colonic metabolism shows the overall progression of
381 the precursors present in wine and the generation of their microbial metabolites during
382 colonic fermentation (Figure 2). Consistent with observations after gastro-intestinal
383 digestion, the behavior of flavanols from both the 2020 and 2021 wines showed similar
384 trends. Both exhibited a similar qualitative profile of microbial metabolites, although
385 there were some variations in their concentrations in the culture medium (Figures 3A-C
386 and Supplemental Tables S2 to S7).

387 Based on the phenol composition of the media after gastro-intestinal digestion (Table
388 2 and Supplemental Tables S2 and S5), it can be inferred that no parent compounds of
389 the wine flavanols enter the AC reactor with the exceptions of catechin, epicatechin and
390 procyanidin B1 at very low concentrations following the digestion of the 2021 wine.
391 However, during the early stage of colonic fermentation (AC), catechin, epicatechin,
392 epigallocatechin, galocatechin and proanthocyanidins were detected (Figure 3A and
393 Supplemental Tables S2 and S5). The concentration of flavanols gradually decrease in
394 TC until completely disappear in DC, with the exception of epigallocatechin,
395 epigallocatechin gallate and procyanidin B1 in wine 2021 (Figures 3A-B). The transient
396 disappearance of flavanols may be explained by non-specific binding interactions of some
397 flavonoids with lipophilic carrier proteins present in the digestion media that could be
398 disrupted by the colonic environment or gut microbiota activity²⁵.

399 The main microbial metabolites detected in the AC section were the benzoic acid
400 related compounds: catechol, pyrogallol and gallic acid (Supplemental Tables S2 & S5).
401 The early appearance of gallic acid may result from the breakdown of more complex
402 molecules and/or the degalloylation of the gallic acid esters of wine flavanols. Other



403 colonic metabolites in the AC were phenyl propionic acid related compounds (Figure 3C).
404 This may indicate the premature microbial degradation of more complex phenolic
405 compounds in the ascending colon.

406 In the TC reactor, a greater abundance and diversity of phenolic species were
407 observed compared to the AC (Figures 3A-C). In the TC section, increases in
408 valerolactones and valeric acids were observed. These are exclusively microbial
409 metabolites of flavanols⁷. In line with that previously described⁷, we identified di- and
410 monohydroxy propan-2-ol, from which hydroxylated valerolactones are generated
411 (Supplemental Tables S3 & S6). The subsequent microbial catabolism of valerolactones
412 produces valeric acid derivatives with varying degrees of hydroxylation, and these were
413 abundant in the TC. Other microbial metabolites detected in the AC, such as *p*-coumaric
414 acid, gallic acid, pyrogallol and catechol, were also detected in the TC at lower
415 concentrations.

416 In the DC section, the predominant compounds included 5-(3,4-dihydroxy phenyl)
417 valerolactone, 5-(3,4-dihydroxy phenyl) valeric acid, 4-hydroxy-5-(4-hydroxy phenyl)
418 valeric acid, benzoic acid related compounds and catechol (Supplemental Tables S4 &
419 S7). The main compounds generated during the colonic fermentation in the DC section
420 belong to the family of phenylpropionic and phenylacetic acids, especially 3-
421 hydroxyphenyl acetic acid and 3(4-hydroxy) phenyl propionic acid (Supplemental Tables
422 S4 & S7). This trend indicates the persistence of these compounds during colonic transit,
423 possibly due to the continuous metabolism of wine flavanols resulting in the formation of
424 valerolactones and valeric acids. These results are consistent with the observations made
425 by Firman et al. (2019)²⁶, where the first colonic segment (AC) exhibited less diversity
426 and abundance of phenolic species compared to the TC and DC. Additionally, our
427 findings align with the same authors' conclusions that the TC and DC have closely related



428 metabolic profiles. Similarly, a study by Cattivelli et al. (2023)¹² showed the degradation
429 driven by the colon microbiota of cooked red-skinned onion flavonols resulted in the
430 accumulation of three main metabolites, i.e., 3-(3'-hydroxyphenyl)propanoic acid, 3-(3'-
431 hydroxyphenyl)acetic acid and 3-(3',4'-dihydroxyphenyl) acetic acid. This provides
432 further evidence of significant colonic metabolism in the TC and DC sections.

433 Given the crucial link between the bioavailability of dietary phenolic compounds
434 and their efficacy as bioactive molecules, numerous *in-vivo* studies have been conducted
435 to elucidate the impact of phenolic microbial metabolites on overall bioavailability²⁷.
436 Considering that flavanols represent the principal phenolic constituents in red wine, the
437 results presented here offer important insights into the association between health
438 benefits, particularly cardiovascular health, and the presence of colonic microbial
439 products derived from wine flavanols. Indeed, the relevance of valerolactones and valeric
440 acid related compounds is evidenced as they have been proposed as intake biomarkers of
441 food containing proanthocyanidins²⁷.

442 **3.3. Impact of wine flavanols on the microbial population and SCFA production**

443 It has been suggested that dietary polyphenols, including those from red wine, can
444 modulate gut microbiota and/or their metabolic activity, positively impacting the
445 reduction of CVD risk factors²⁸. In this work, the plate counting technique was used to
446 examine variations in viable gut bacteria in the media of the AC, TC and DC during the
447 stabilization period (days 0, 5, 7 and 12) and during the wine treatment period (days 14,
448 19, 21 and 26) (Figure 1). During the initial phase of stabilization, the fecal bacteria
449 introduced adapted to each reactor according to the characteristics of the media, such as
450 pH and nutrient availability²⁶. In our study (Figure 4), during the wine treatment period,
451 (days 14, 19, 21 and 26), *Bifidobacterium* gradually increased in the three colon sections
452 except in AC with wine 2021 treatment (Figure 4A). In contrast, the count of



453 *Enterobacter* tended to decrease in the three reactors, particularly evident during the
454 treatment period of with wine 2021 (Figure 4). Finally, there were no evident changes in
455 the count of *Lactobacillus* in the AC, TC and DC during the treatment period with wine
456 2021, contrary, the treatment with wine 2020 tended to increase this bacteria population
457 in the three reactors (Figure 4). In contrast to the differences observed for microbial
458 metabolites profile of flavanols in the three reactors during colonic fermentation, no
459 marked differences were observed in *Bifidobacterium*, *Enterobacter* and *Lactobacillus*
460 counts between the culture mediums of AC, TC and DC (Figure 4).

461 SCFA are microbial products derived from the anaerobic fermentation of non-
462 absorbed dietary compounds, especially carbohydrates and, to a lesser extent, dietary and
463 endogenous proteins²⁹. Chromatographic analysis of the culture medium from the AC,
464 TC and DC, respectively, collected at the baseline (stabilization period, day 12) and at
465 the end of the wine treatment period (day 26) (Figure 1) showed that wine
466 supplementation modulates the production rate of SCFA (Figure 5). In both wines (2020
467 and 2021), the most marked change was the increase in the production of butyric and
468 propionic acids in the TC and DC (Figures 5B & 5C). Regarding acetic acid, we observed
469 that its production was stimulated during the incubation of wine 2021 in all the reactors
470 but not with wine 2020. Since acetic and butyric acids share a common metabolic
471 pathway, it is suggested that the presence of red wine may favor the synthesis of butyric
472 acid at the expense of acetic acid^{26,29}. This effect on the stimulation of butyric and
473 propionic acids production may also be due to a direct interaction of phenolic metabolites
474 with bacterial activity or a direct interaction of these compounds in the metabolism of
475 these SCFA. These results concord with a recent study²³, in which the production of
476 butyric acid was significantly higher when red wine was fermented alone compared to
477 when it was combined with a lipid food model, suggesting that the non-bioavailable



478 fraction resulting from wine digestion could potentiate the production of butyric acid
479 Conversely, Suo et al. (2021)³⁰ did not observe differences in the generation of various
480 SCFA classes when fermenting isolated high-molecular-weight-polyphenolic complexes
481 and oligomeric phenols compared with control (deionized water). This indicates that wine
482 as a whole entity may play a role in the generation of butyric acid rather than isolated
483 (poly)phenols. Extensive research has investigated the role of SCFA in human health,
484 with particular emphasis on butyric acid due to its significant impact on various
485 physiological processes in the human body³¹.

486 **3.4. Study of the potential cardioprotective activity of wine flavanol microbial** 487 **metabolites in cell line models**

488 CVD comprises a spectrum of disorders, including coronary artery disease, stroke,
489 hypertension and heart failure. Many researchers have identified a positive association
490 between moderate red wine intake and an improvement in cardiovascular health
491 parameters. Over the last decade, research has emphasized the role of the microbiome in
492 regulating cardiovascular physiology and disease progression. These findings highlight
493 the importance of identifying whether microbial metabolites produced from wine
494 polyphenols contribute to the observed health effects. Understanding the interplay
495 between wine polyphenols, gut microbiota, and cardiovascular health could provide
496 valuable insights for uncovering novel therapeutic strategies aimed at preventing and
497 managing CVD. In order to study the cardio-protective effect of microbial metabolites,
498 culture medium from the AC, TC and DC collected at the baseline (stabilization period
499 day 12) and at the end of the wine treatment period (day 26) (Figure 1), containing the
500 wine flavanol microbial metabolites, were exposed to endothelial and hepatic cell models.

501 *3.4.1. Cell viability assessment*



502 A fluorometric assay was performed to assess the potential toxicological impact of
503 colonic fermentation media. Based on the cell viability assay performed on EA.hy926
504 endothelial and HepG-2 hepatic cells treated for 24 hours with culture medium from the
505 AC, TC and DC compartments (Figure 1), a dilution of 1/8 was selected to study the
506 functionality of colonic metabolites as this dilution exhibited no cytotoxicity towards the
507 cells (data not shown).

508 *3.4.2. Effect of wine flavanol colonic metabolites on NO levels and endothelin (END-1)* 509 *expression in HepG2 cells*

510 Endothelial cells were utilized to assess the impact of flavanol microbial metabolites
511 present in the three colonic culture medium (AC, TC and DC) on vascular tone regulation.
512 We focused on two key vasoactive substances released from the endothelium: nitric oxide
513 (NO) and endothelins (ETs). While NO exerts potent vasodilatory effects, ETs are among
514 the most potent vasoconstrictors. In the present study, we investigated the release of NO
515 and the expression level of mRNA END-1, observing significant statistical differences
516 between cells incubated with the stabilization media at 12 days (basal) and the wine-
517 fermented media at 26 days (wine treatment period) ($p < 0.05$) (Figure 6). Specifically, the
518 production of NO in cells incubated with the media containing the microbial metabolites
519 (wine treatment) was significantly higher than in the stabilization media (basal) in the
520 three reactors for the 2020 and 2021 wines. The level of mRNA of ET-1 increased
521 significantly in all the reactors, except for the TC after the 2021 wine treatment (Figure
522 6B). Consistent with previous research, changes in the END-1 concentration in cells
523 demonstrated an inverse association with the NO concentration, maintaining proper
524 vascular tone balance and preventing endothelial cell dysfunction³².

525 *3.4.3. Modulation of cholesterol metabolism and insulin resistance in treated-HepG2* 526 *cells with wine flavanol colonic metabolites*



527 Another risk factor for cardiovascular disease is the level of lipids, particularly LDL^{New Article Online}
528 cholesterol. Therefore, we explored the potential of the wine flavanol microbial
529 metabolites present in the culture medium from the AC, TC and DC, before and after
530 wine treatment, to influence the expression of the LDL receptor (LDLr) and HMG-CoA
531 in the hepatic cell line, both of which are involved in cholesterol biosynthesis. This study
532 revealed that the culture medium collected from the three reactors during both wines
533 treatment (2020 and 2021) can enhance the expression level of mRNA LDLr (Figure 7A),
534 thereby facilitating the removal of LDL cholesterol from circulation³³. This effect can be
535 attributed to the presence of several wine flavanol microbial metabolites in the culture
536 medium.

537 The regulation in the expression of mRNA HMGCo-A showed differences between
538 the wines from 2020 and 2021 (Figure 7B). In this instance, only cells exposed to the
539 culture medium from the TC and DC of the 2021 wine showed a significant down-
540 regulation in the expression of mRNA HMGCo-A, contributing with the inhibitory effect
541 of cholesterol biosynthesis in the liver. Previous research has found an inverse
542 relationship between the mRNA abundance of HMG-CoA reductase and LDLr mRNA³⁴.
543 These results suggest that microbial metabolites generated by colonic fermentation of
544 wine flavanols stimulate the expression of the LDLr gene (Figure 7A), whereas transcript
545 levels of HMG-CoA were not significantly affected by the wine treatment (Figure 7B),
546 and these may depend on the concentration of microbial metabolites rather than the
547 composition.

548 Regarding insulin resistance, a risk in CVD, the liver plays a pivotal role in
549 regulating blood glucose levels through various processes including gluconeogenesis,
550 glycogen synthesis, and glycogen breakdown. AKT, a key mediator in the PI3K/AKT
551 signaling pathway, exerts influence over these metabolic processes. Reduced AKT levels



552 can hinder glucose transportation and disrupt glycogen synthesis, potentially resulting in
553 elevated blood glucose levels and insulin resistance³⁵. In the present study, the hepatic
554 cells exposed to the culture medium of the AC, TC and DC from microbial fermentation
555 of the 2020 and 2021 wines reduced the risk of insulin resistance, disrupting glycogen
556 synthesis (Figure 8A) and inhibiting hepatic glucose generation by down-regulation of
557 mRNA AKT expression (Figure 8B). These findings suggest that wine flavanol microbial
558 metabolites can modulate hepatic glucose metabolism, thereby potentially offering
559 therapeutic benefits in managing insulin resistance and glycemic control. In addition to
560 microbial metabolites, the SCFA present in the fermentation culture medium (AC, TC
561 and DC), could modulate the CVD risk parameters studied. Previous data showed that
562 butyric acid modulates insulin resistance and the accumulation of fat in the liver¹¹. In
563 addition, the increment in the plasma levels of butyric acid has been associated with an
564 improvement of the endothelial function³⁶.

565 In conclusion, the results of the present study show that wine flavanols, submitted to
566 a dynamic *in-vitro* digestion model, reach the colon where they are transformed by the
567 colon microbiota. The colonic fermentation of wine flavanols resulted in the
568 accumulation of three main metabolites, i.e., 3-(3'-hydroxyphenyl)propanoic acid, 3-(3'-
569 hydroxyphenyl)acetic acid and 3-(3',4'-dihydroxyphenyl)acetic acid. In addition, an
570 increase in a complex mixture of valerolactone and valeric acid derivatives was observed
571 in the TC and DC sections. In parallel, a significant increase in the production of butyric
572 and propionic acids was observed respectively in the TC and DC, and an increase in the
573 count of certain bacteria, mainly *Bifidobacterium*. The functionality study shows that
574 exposing fermentation media, containing the wine flavanol microbial metabolites, to
575 endothelial and hepatic cell lines positively modulates four biomarkers associated with
576 three CVD risk factors. Specifically, an increase was observed in the vasodilator NO that



577 improves the blood pressure. In addition, there was an improvement in the LDL receptors
578 and the HMGCoA enzyme, with a positive effect on the cholesterol metabolism, with the
579 reduction of glycogen levels improving insulin resistance. The results of this study
580 reinforce the idea that wine flavanols are intensively metabolised by colonic microbiota
581 to generate a complex mixture of their bioactive forms that could influence host health.

582 **Acknowledgements**

583 This study was supported by the MCIN (Ministerio de Ciencia e Innovación) through the
584 CDTI project IDI-20210434. Silvia Yuste has a Margarita Salas postdoctoral grant funded
585 by the European Union-NextGenerationEU through the Ministerio de Universidades and
586 the Universitat de Lleida. The authors are grateful to the technical staff of the Instrumental
587 Analysis Service at the ICVV for their UHPLC-QqQ-MS/MS analytical support.

588 **Conflicts of interest**

589 On behalf of all the authors, the corresponding author states that there is no conflict of
590 interest.

591 **Contributions**

592 **Juana Mosele**: Formal analysis, Investigation, Writing -original draft, Writing - review
593 & editing; **Blanca Viadel**: Conceptualization, Project administration, Validation Data
594 curation, Formal analysis, Investigation, Methodology, Software; **Silvia Yuste**: Formal
595 analysis, Investigation, Methodology; **Lidia Tomás-Cobos**: Formal analysis,
596 Investigation, Methodology; **Sandra García**: Formal analysis, Investigation,
597 Methodology; **María-Teresa Escribano Bailón**: Conceptualization, Data curation,
598 Formal analysis, Investigation; **Ignacio García Estévez**: Conceptualization, Data
599 curation, Formal analysis, Investigation; **Pilar Moretón Fraile**: Conceptualization,
600 Funding acquisition, Project administration; **Fernando Rodríguez de Rivera**:



601 Conceptualization, Funding acquisition, Project administration; **Soledad de Domingo**
602 **Casado**: Conceptualization, Funding acquisition, Project administration; **Maria-Jose**
603 **Motilva**: Investigation; Methodology, Writing -original draft, and Writing - review &
604 editing.

605 **References**

- 606 1. R. G. Ntuli, Y. Saltman, R. Ponangi, D. W. Jeffery, K. Bindon and K. L. Wilkinson.
607 Impact of fermentation temperature and grape solids content on the chemical
608 composition and sensory profiles of Cabernet Sauvignon wines made from flash
609 détente treated must fermented off-skins, *Food Chem.*, 2022, **369**, 130861.
- 610 2. I. Buljeta, A. Pichler, J. Šimunović and M. Kopjar. Beneficial Effects of Red Wine
611 Polyphenols on Human Health: Comprehensive Review, *Curr Issues Mol Biol.*, 2023,
612 **45**, 782-798.
- 613 3. X. Zhang, X. Song, X. Hu, F. Chen, and C. Ma. Health benefits of proanthocyanidins
614 linking with gastrointestinal modulation: An updated review, *Food Chem.*, 2022,
615 134596.
- 616 4. G. Raman, M. Shams-White, E. E. Avendano, F. Chen, J. A. Novotny and A. Cassidy,
617 A. Dietary intakes of flavan-3-ols and cardiovascular health: a field synopsis using
618 evidence mapping of randomized trials and prospective cohort studies, *Syst Rev.*, 2018,
619 **7**, 100.
- 620 5. F. Castello, G. Costabile, L. Bresciani, M. Tassotti, D. Naviglio, D. Luongo, P. Ciciola,
621 M. Vitale, C. Vetrani, G. Galaverna, F. Brighenti, R. Giacco, D. Del Rio, and P. Mena.
622 Bioavailability and pharmacokinetic profile of grape pomace phenolic compounds in
623 humans, *Arch Biochem Biophys*, 2018, **646**, 1–9.



- 624 6. S. Yuste, I. A. Ludwig, L. Rubi , M. P. Romero, A. Pedret, R. M. Valls, ... and A. Maci , A. In vivo biotransformation of (poly) phenols and anthocyanins of red-fleshed
625 apple and identification of intake biomarkers, *J Funct Foods*, 2019, **55**, 146-155. DOI: 10.1039/D4FO03774J
- 626
- 627 7. J. I. Mosele, A. Maci , M. P. Romero, M. J. Motilva, and Rubi , L. Application of in
628 vitro gastrointestinal digestion and colonic fermentation models to pomegranate
629 products (juice, pulp and peel extract) to study the stability and catabolism of phenolic
630 compounds, *J Funct Foods*, 2015, **14**, 529-540.
- 631 8. M. J. Cires, P. Navarrete, E. Pastene, C. Carrasco-Pozo, R. Valenzuela, D. Medina, A.
632 ... and M. Gotteland, Effect of a proanthocyanidin-rich polyphenol extract from
633 avocado on the production of amino acid-derived bacterial metabolites and the
634 microbiota composition in rats fed a high-protein diet, *Food Funct.*, 2019, **10**, 4022-
635 4035.
- 636 9. M. Monagas, M. Urpi-Sarda, F. S nchez-Pat n, R. Llorach, I. Garrido, G mez-
637 Cordov s, C. ... and Bartolome, B. Insights into the metabolism and microbial
638 biotransformation of dietary flavan-3-ols and the bioactivity of their metabolites, *Food*
639 *Funct.*, 2010, **1**, 233-253.
- 640 10. M. A. Polewski, D. Esquivel-Alvarado, N. S. Wedde, C. G Kruger, and J. D. Reed.
641 Isolation and characterization of blueberry polyphenolic components and their effects
642 on gut barrier dysfunction, *J Agric Food Chem.*, 2019, **68**, 2940-2947.
- 643 11. X. Zhao, Y. Wu, H. Liu, N. Hu, Y. Zhang, and S. Wang. Grape seed extract
644 ameliorates PhIP-induced colonic injury by modulating gut microbiota, lipid
645 metabolism, and NF- B signaling pathway in rats, *J Funct Foods*, 2021, **78**, 104362.
- 646 12. A. Cattivelli, L. Nissen, F. Casciano, D. Tagliazucchia, and A. Gianotti. Impact of
647 cooking methods of red-skinned onion on metabolic transformation of phenolic
648 compounds and gut microbiota changes, *Food Funct.*, 2023, **14**, 3509–3525.



- 649 13. L. Nissen, A. Cattivelli, F. Casciano, A. Gianotti, and D. Tagliazucchi. Roasting and
650 frying modulate the phenolic profile of dark purple eggplant and differently change
651 the colon microbiota and phenolic metabolites after *in vitro* digestion and fermentation
652 in a gut model. *Food Res. Int.*, 2022, **160**, 111702. View Article Online
DOI: 10.1039/D4FO03774J
- 653 14. R.A. Kemperman, S. Bolca, L.C. Roger, and E. E. Vaughan. Novel approaches for
654 analysing gut microbes and dietary polyphenols: challenges and opportunities,
655 *Microbiology*, 2010, **156**, 3224–3231.
- 656 15. I., García-Estévez, C. Alcalde-Eon, and M. T. Escribano-Bailón. Flavanol
657 quantification of grapes via multiple reaction monitoring mass spectrometry.
658 application to differentiation among clones of *Vitis Vinifera* L. cv Rufete grapes, *J*
659 *Agric Food Chem.*, 2017, **65**, 6359–6368.
- 660 16. J. A. Nieto, C Rosés, P. García-Ibáñez, B. Pérez, B. Viadel, A. Romo-Hualde, F. I.
661 Milagro, A. Barceló, M. Carvajal, E. Gallego, and A. Agudelo. Fiber from elicited
662 butternut pumpkin (*Cucurbita moschata* D. cv. Ariel) modulates the human intestinal
663 microbiota dysbiosis, *Int J Biol Macromol.*, 2024, **269** (Pt 2):132130.
- 664 17. P. Marteau, B. Flourié, P. Pocharb, C. Chastang, J.F. Desjeux, and J.C. Rambaud.
665 Effect of the microbial lactase (*EC 3.2.123*) activity in yoghurt on the intestinal
666 absorption of lactose: An in vivo study in lactase-deficient humans. *British J. Nut.*,
667 1990, **64**, 71-79.
- 668 18. C. Rosès, B. Viadel, J. A. Nieto, L. Soriano-Romaní, A. Romo-Hualde, A. Agudelo,
669 F.I. Milagro and A. Barceló. Gut microbiota modulatory capacity of *Brassica oleracea*
670 *italica* x *alboglabra* (Bimi®), *Food Biosci.*, 2023, **55**, 103006, 2212-4292.
- 671 19. C. Roses, J. A. Nieto, B. Viadel, E. Gallego, A. Romo-Hualde, S. Streitenberger, F.
672 I. Milagro, A. Barceló, E. F. Vieira, and C. Soares. An in vitro protocol to study the



- 673 modulatory effects of a food or biocompound on human gut microbiome and
674 metabolome, *Foods*, 2021, **10**, 3020. View Article Online
DOI: 10.1039/D4FO03774J
- 675 20. K. Molly, M. Vande Woestyne, I. De Smet, and W. Verstraete. Validation of the
676 Simulator of the Human Intestinal Microbial Ecosystem (SHIME) Reactor Using
677 Microorganism-Associated Activities, *Microb. Ecol. Health Dis.*, 1994, **7**, 191–200.
- 678 21. K. Molly, M. Vande Woestyne and W. Verstraete. Development of a 5-Step Multi-
679 Chamber Reactor as a Simulation of the Human Intestinal Microbial Ecosystem, *Appl*
680 *Microbiol Biotechnol*, 1993, **39**, 254–258.
- 681 22. C. Royo, Y. Ferradás, J. M. Martínez-Zapater and M. J. Motilva. Characterization of
682 Tempranillo negro (VN21), a high phenolic content grapevine Tempranillo clone,
683 through UHPLC-QqQ-MS/MS polyphenol profiling, *Food Chem.*, 2021, **360**, 130049.
- 684 23. A. Tamargo, D. G. de Llano, C. Cueva, J. N. Del Hierro, D. Martin, N. Molinero, B.
685 Bartolomé and V. Moreno-Arribas. Deciphering the interactions between lipids and
686 red wine polyphenols through the gastrointestinal tract, *Food Res Int.*, 2023, **165**,
687 112524.
- 688 24. J. Liang, S. Yang, Y. Liu, H. Li, M. Han and Z. Gao. Characterization and stability
689 assessment of polyphenols bound to *Lycium barbarum* polysaccharide: Insights from
690 gastrointestinal digestion and colon fermentation, *Food Res. Int.*, 2024, **179**, 114036
- 691 25. P. M. Joyner. Protein Adducts and Protein Oxidation as Molecular Mechanisms of
692 Flavonoid Bioactivity, *Molecules*, 2021, **26**, 5102.
- 693 26. J. Firman, L. Liu, C. Tanes, E. S. Friedman, K. Bittinger, S. Daniel, P. van den
694 Abbeele and B. Evans. Metabolic Analysis of Regionally Distinct Gut Microbial
695 Communities Using an *In Vitro* Platform, *J Agric Food Chem.*, 2020, **68**, 13056–
696 13067.



- 697 27. P. Mena, I. A. Ludwig, V. B. Tomatis, A. Acharjee, L. Calani, A. Rosi, F. Brighenti,
698 S. Ray, J. L. Griffin, L. J. Bluck, and D. Del Rio. Inter-individual variability in the
699 production of flavan-3-ol colonic metabolites: preliminary elucidation of urinary
700 metabolotypes, *Eur J Nutr*, 2019, **58**, 1529–1543.
- 701 28. W. H. W. Tang, F. Bäckhed, U. Landmesser and S. L. Hazen. Intestinal Microbiota in
702 Cardiovascular Health and Disease: JACC State-of-the-Art Review, *J Am Coll Card.*,
703 2019, **73**, 2089–2105.
- 704 29. S. Macfarlane and G. T. Macfarlane. Regulation of short-chain fatty acid production,
705 *Proceedings Nutr Soc*, 2003, **62**, 67–72.
- 706 30. H. Suo, M. R. I. Shishir, J. Xiao, M. Wang, F. Chen, and K. W. Cheng. Red Wine
707 High-Molecular-Weight Polyphenolic Complex: An Emerging Modulator of Human
708 Metabolic Disease Risk and Gut Microbiota, *J Agric Food Chem.*, 2021, **69**, 10907–
709 10919.
- 710 31. D. J. Morrison and T. Preston. Formation of short chain fatty acids by the gut
711 microbiota and their impact on human metabolism, *Gut Microbes*, 2016, **7**, 189–200.
- 712 32. S. Kuruppu N. W. Rajapakse R. A. Dunstan and A. I. Smith. Nitric oxide inhibits the
713 production of soluble endothelin converting enzyme-1, *Mol Cell Biochem.*, 2014, **396**,
714 49-54.
- 715 33. K. Ioriya, K. Kino, S. Horisawa, T. Nishimura, M. Muraoka, T. Noguchi, and N.
716 Ohashi. Pharmacological profile of SMP-797, a novel acyl-coenzyme a: cholesterol
717 acyltransferase inhibitor with inducible effect on the expression of low-density
718 lipoprotein receptor, *J Cardiovasc Pharmac.*, 2006, **47**, 322–329.
- 719 34. I. J. Cho, J. Y. Ahn, S. Kim, M. S. Choi and T. Y. Ha. Resveratrol attenuates the
720 expression of HMG-CoA reductase mRNA in hamsters, *Biochem Biophysical Res
721 Communic.*, 2008, **367**, 190–194.



- 722 35. M. Li, X. Chi, Y. Wang, S. Setrerrahmane, W. Xie and H. Xu. Trends in insulin View Article Online
DOI: 10.1039/D4FO03774J
- 723 resistance: insights into mechanisms and therapeutic strategy, *Signal Transduction*
- 724 *Target Therapy*, 2022, **7**, 216.
- 725 36. Q. Tian, F. P. Leung, F. M, Chen, X. Y. Tian, Z. Chen, G. Tse, S. Ma, and W. T.
- 726 Wong, Butyrate protects endothelial function through PPAR δ /miR-181b signaling,
- 727 *Pharmacol Res.*, 2021, **169**,105681.
- 728



729 **Figure Captions**

730 **Figure 1.** Scheme of the experimental protocol of the in-vitro gastrointestinal digestion
731 and colonic fermentation of red wine. G: gastric digestion step, I: intestinal digestion step,
732 AC: ascending colon section, TC: transversal colon section, DC: descending colon
733 section, SCFA: short chain fatty acids. Bold numbers are the days of sampling media
734 from the reactors during stabilization (0-12 days) and treatment (13-26 days) periods,
735 respectively. The dashed circles indicate the days of sampling media to microbiota
736 analysis during stabilization (days 0, 5, 7, 12 days) and treatment (days 14, 19, 21, 26)
737 periods, and to SCFA and cell culture assays at the end of the stabilization (day 12) and
738 treatment (day 26) periods. The squares indicate the days of sampling media to
739 chromatographic analysis (UHPLC-MS/MS) of flavanoid metabolites at the end of the
740 stabilization (day 12) and during the treatment (days 13, 14, 15, 16, 18, 20, 23 and 26)
741 periods, respectively.

742
743 **Figure 2.** Kinetic disappearance of total flavanols (precursors) of the wines from 2020
744 (solid blue line) and 2021 (dashed blue line) harvests, and the parallel production of
745 flavanol colonic metabolites (solid purple line and discontinued purple line for wines
746 from 2020 and 2021, respectively) during the dynamic *in-vitro* colonic fermentation. AC:
747 ascending colon, TC: transversal colon, DC: descending colon. Data are expressed as
748 mean (n = 2).

749
750 **Figure 3.** Kinetic disappearance of flavanol monomers (A) and oligomers (B) of wines
751 from 2020 (solid line) and 2021 (dashed line) harvests, and microbial metabolites
752 production (C) during the dynamic *in-vitro* colonic fermentation. AC: ascending colon,
753 TC: transversal colon, DC: descending colon. Data are expressed as mean (n = 2).



754 **Figure 4.** Bacteria abundance in culture medium (A) AC: ascending colon, (B) TC
755 transversal colon, (C) DC: descending colon, sampled at different days of the stabilization
756 period (days 0, 5, 7 and 12 in lighter colour) and wine treatment period (days 14, 19, 21
757 and 26). Wines from 2020 (solid bars) and wines from 2021 (grid fill). Data are expressed
758 as mean \pm SD (n = 2).

759
760 **Figure 5.** Amount of short chain fatty acids quantified in (A) AC: ascending colon, (B)
761 TC: transversal colon and (C) DC: descending colon at the beginning (basal, day12) and
762 at the end of the treatment (day 26) period after the supplementation with wines from
763 2020 (solid bars) and 2021(grid bars). Data are expressed as mean \pm SD (n = 2).

764
765 **Figure 6.** Evaluation of endothelial function parameters through (A) nitric oxide (NO)
766 production and (B) expression levels of nitric oxide synthase (ENDT) mRNA in
767 EA.hy926 cells exposed to media obtained from different colonic reactors representing
768 the ascending colon (AC), transversal colon (TC) and descending colon (DC) sections,
769 before and after wine 2020 (purple solid bars) and 2021 (purple grid bars)
770 supplementation. Data are expressed as mean \pm SD (n = 4). *p < 0.05; ***p < 0.001;
771 ****p < 0.0001 respect to control.

772
773 **Figure 7.** Cholesterol metabolism evaluated by expression levels of (A) LDL receptor
774 mRNA and (B) HMGCo-R mRNA in HepG2 cells exposed to media obtained from
775 different colonic reactors representing the ascending colon (AC), transversal colon (TC)
776 and descending colon (DC) before and after wine 2020 (purple solid bars) and 2021
777 (purple grid bars) supplementation. Data are expressed as mean \pm SD (n = 4). *p < 0.05;
778 **p < 0,005; ****p < 0,0001 respect to control.



779 **Figure 8.** Carbohydrate metabolism evaluation by (A) synthesis of glycogen and (B)
780 expression levels of Akt mRNA in HepG2 cells exposed to media obtained from different
781 colonic reactors representing the ascending colon (AC), transversal colon (TC) and
782 descending colon (DC) before and after wine 2020 (purple solid bars) and 2021 (purple
783 grid bars) supplementation. Data are expressed as mean \pm SD (n = 4). *p < 0.05; ****p
784 < 0.0001 respect to control.

View Article Online
DOI: 10.1039/D4FO03774J



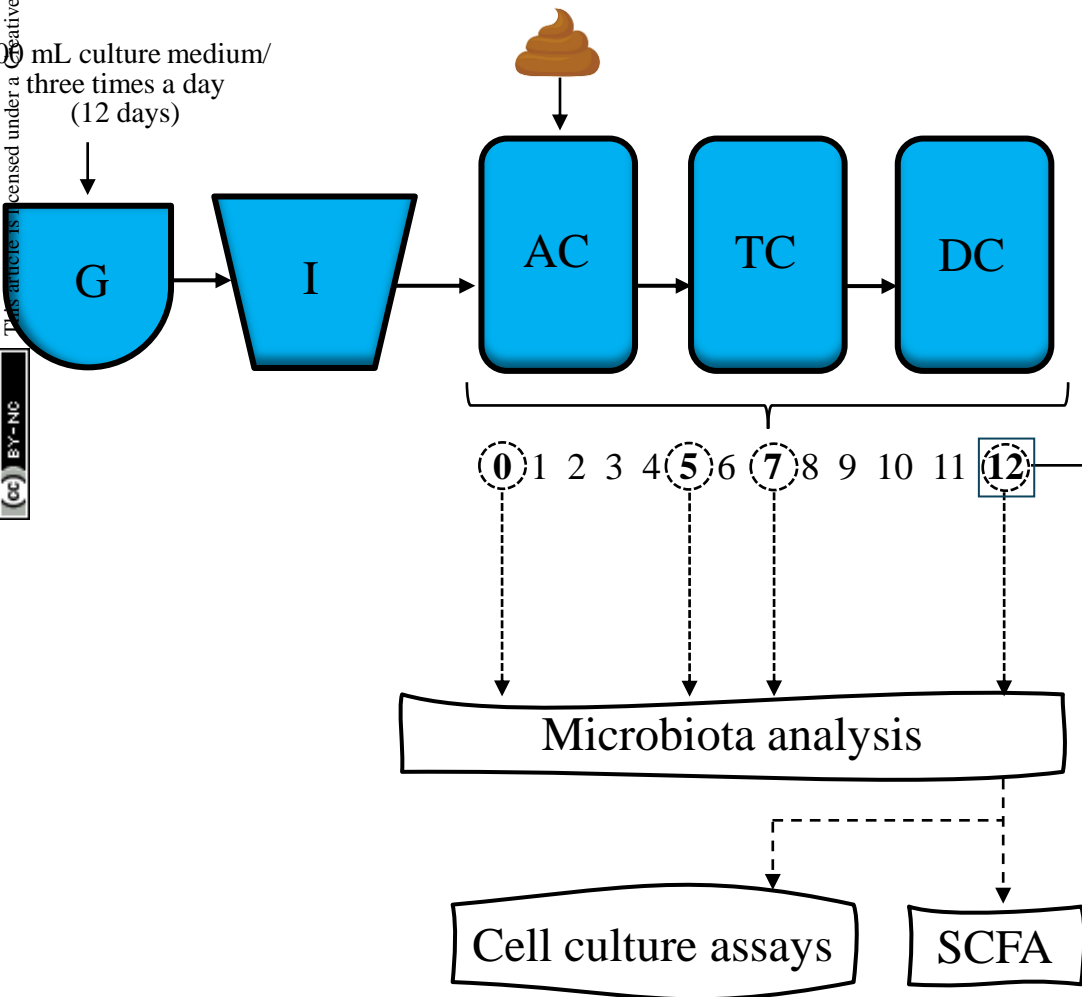
Data Availability Statement

View Article Online
DOI: 10.1039/D4FO03774J

The data supporting this article have been included as part of the Supplemental Information (Figure S1 and Tables S1-S7)



STABILIZATION PERIOD (0-12 days)



WINE TREATMENT PERIOD (13-26 days)

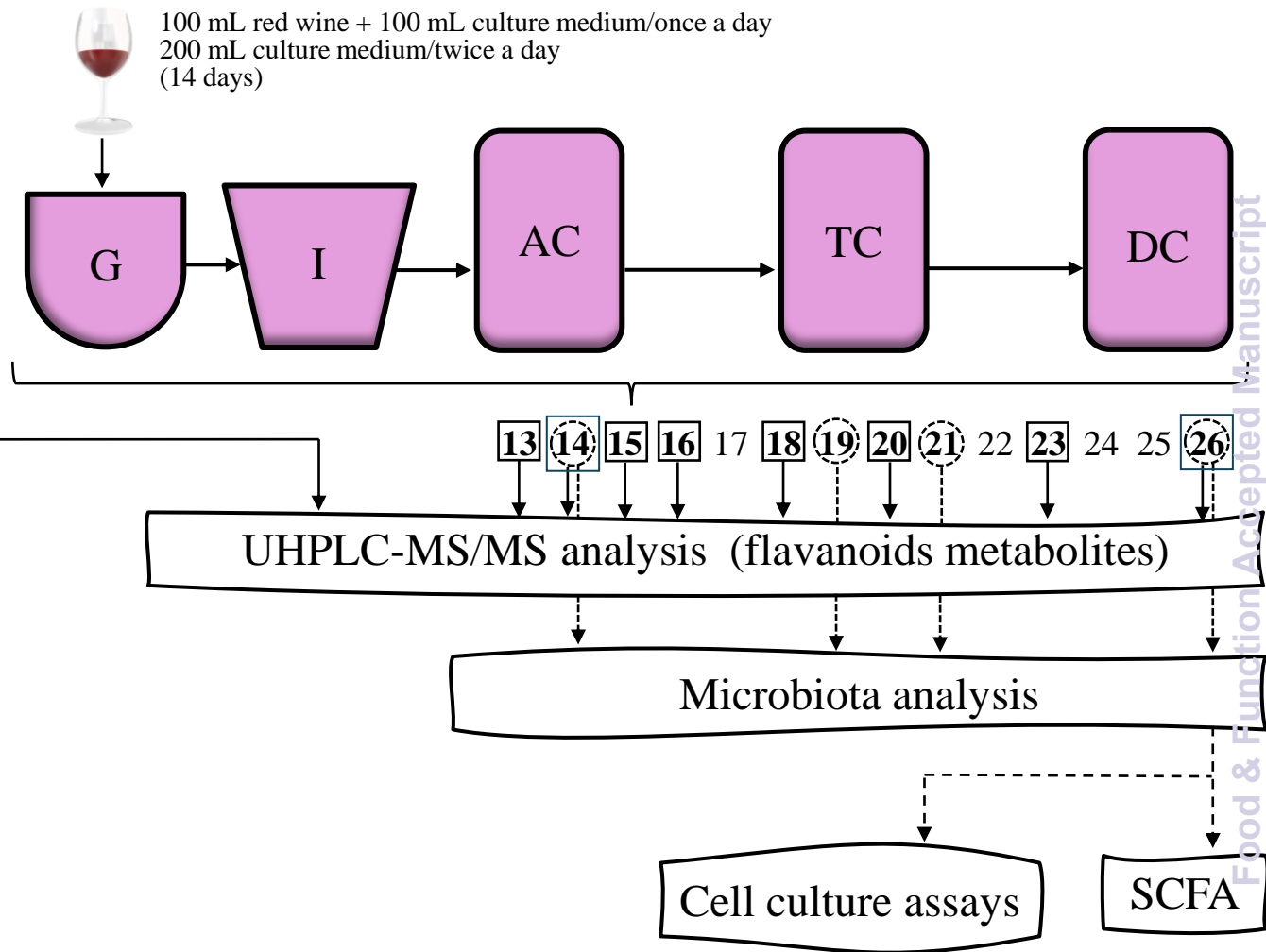


Figure 1

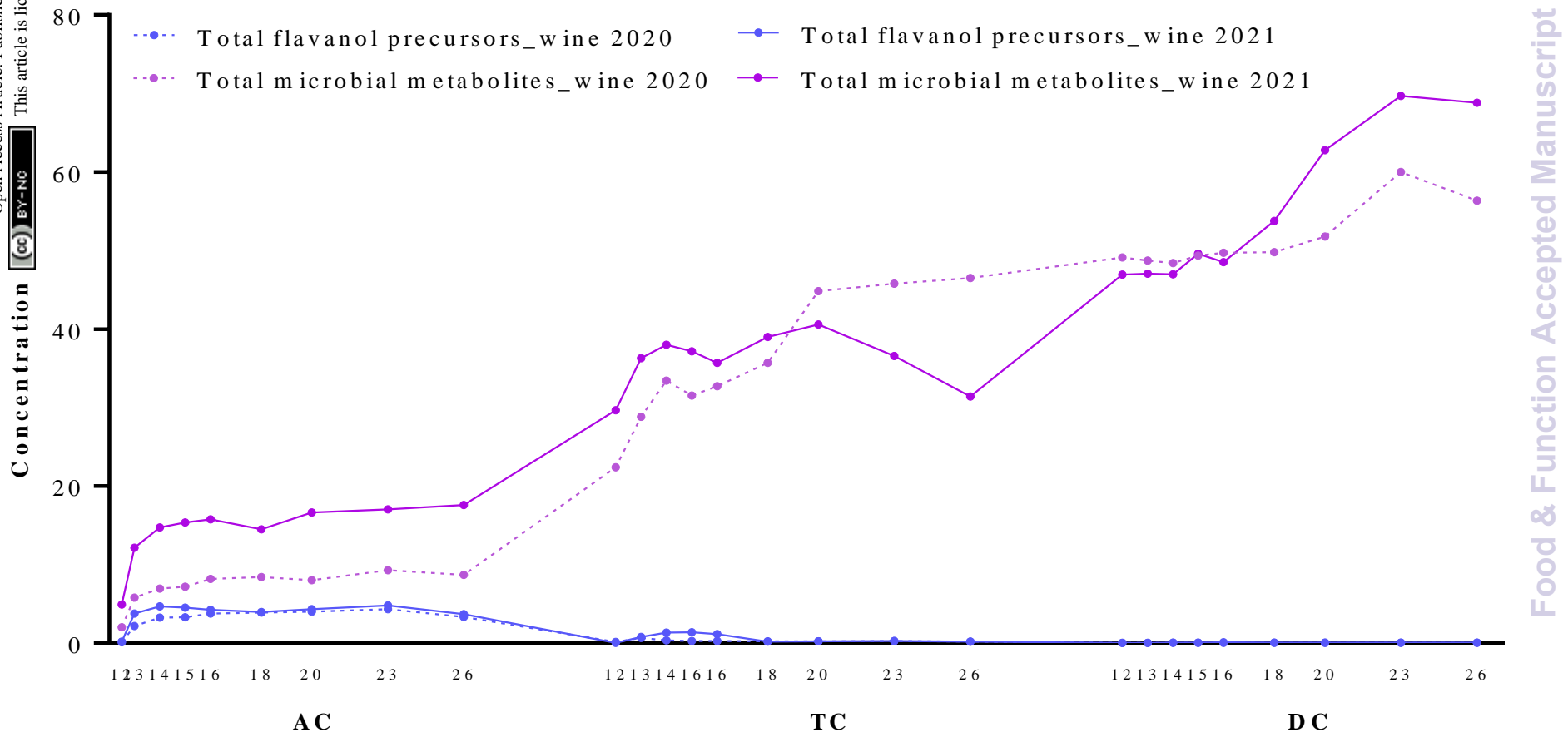
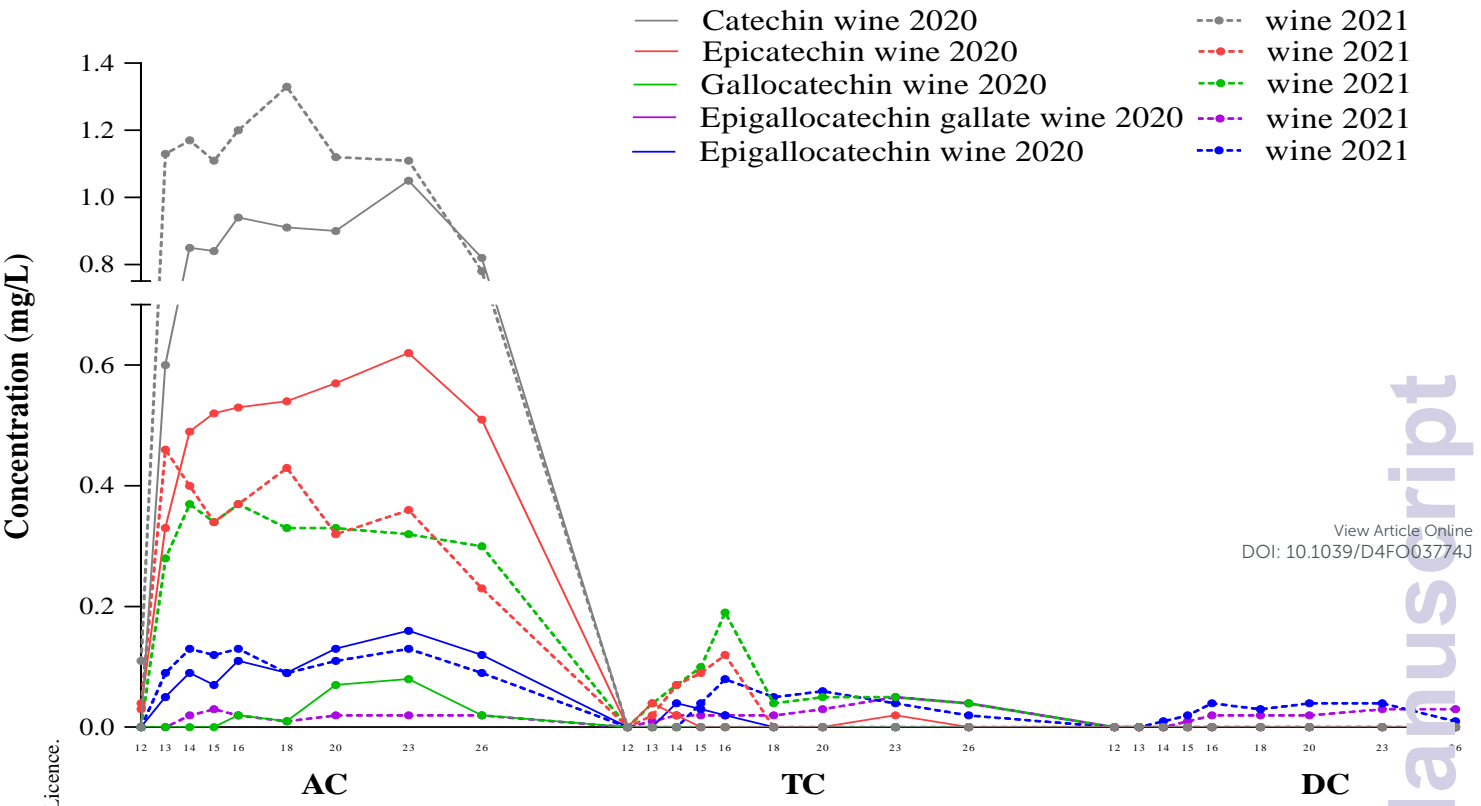


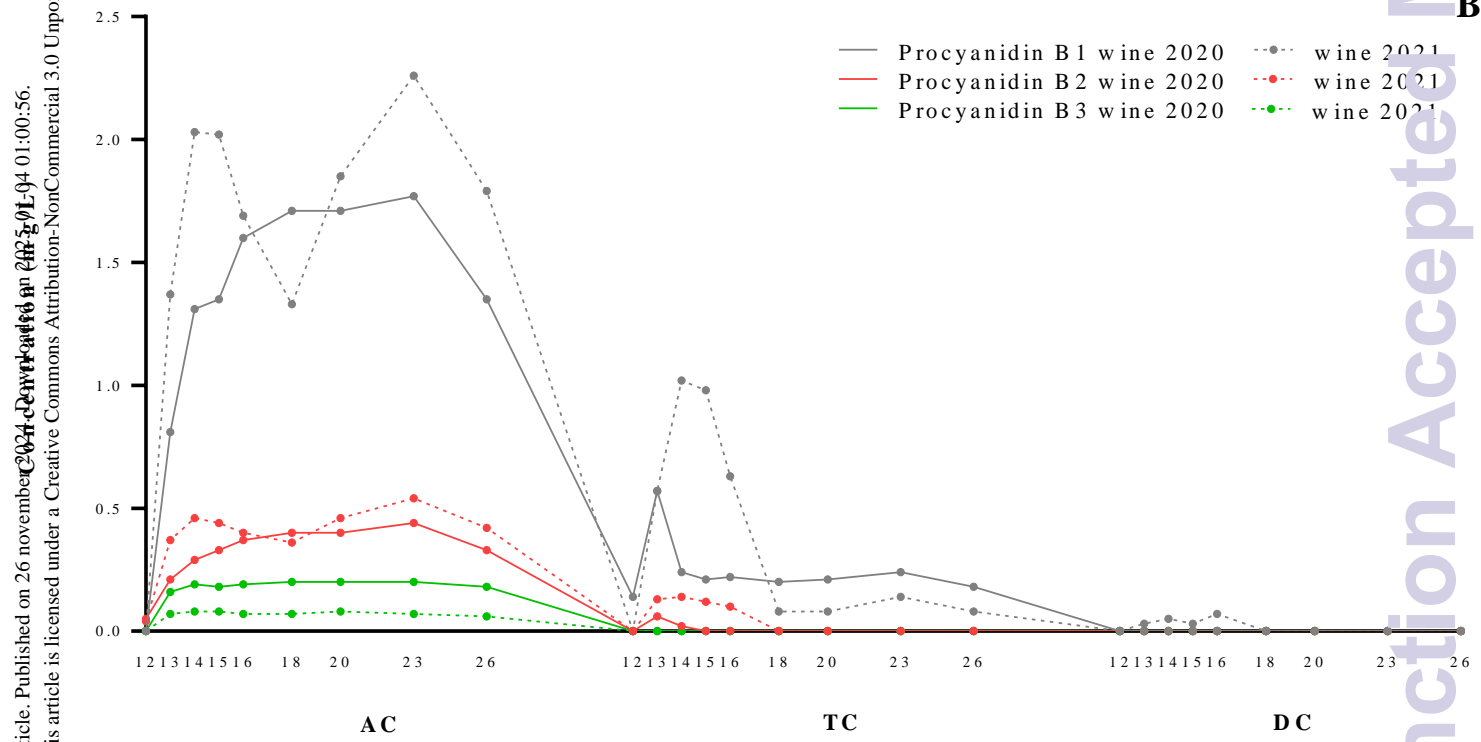
Figure 2

Figure 3

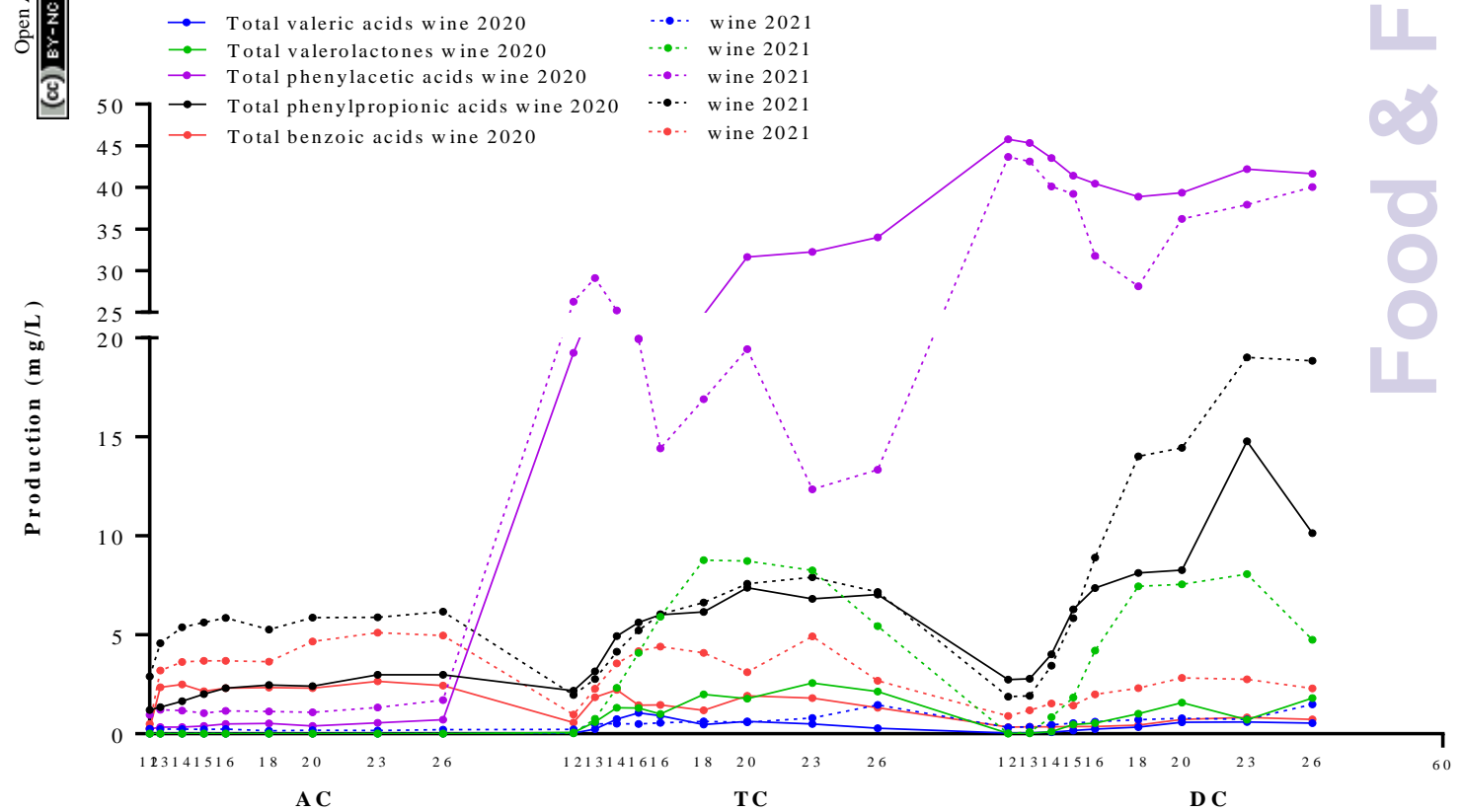
A



B



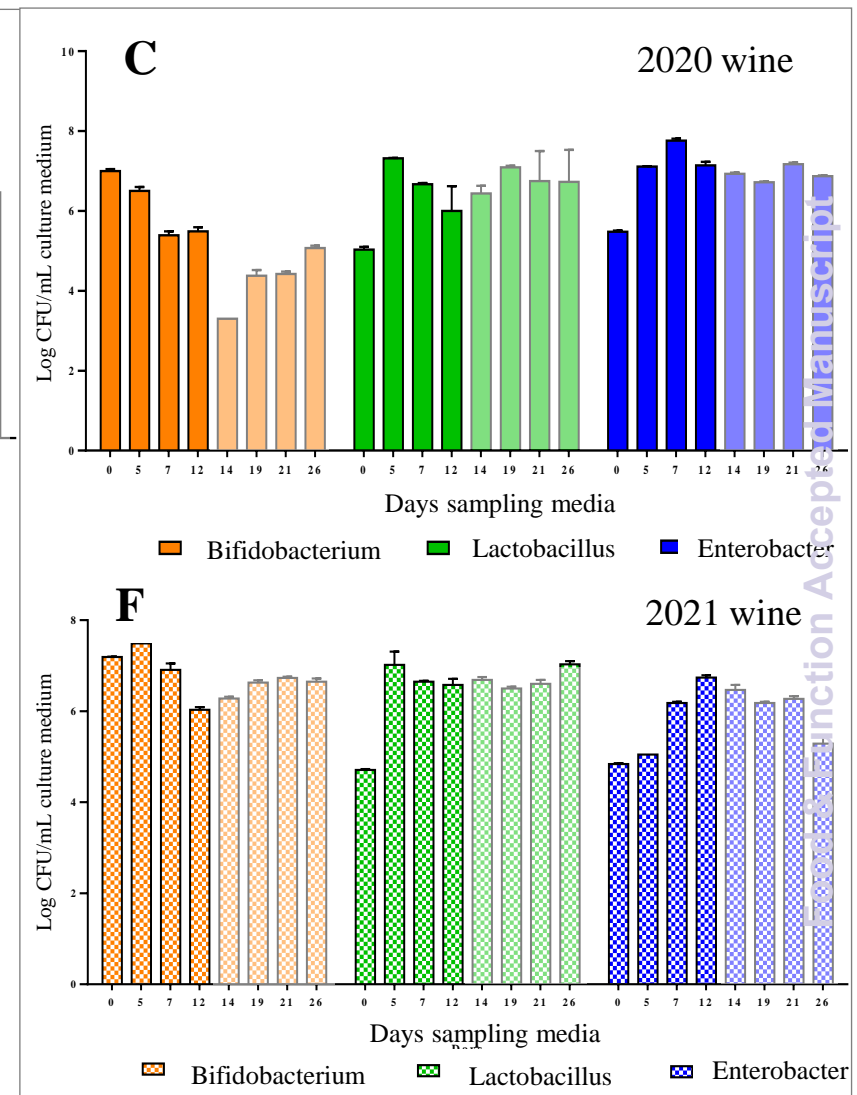
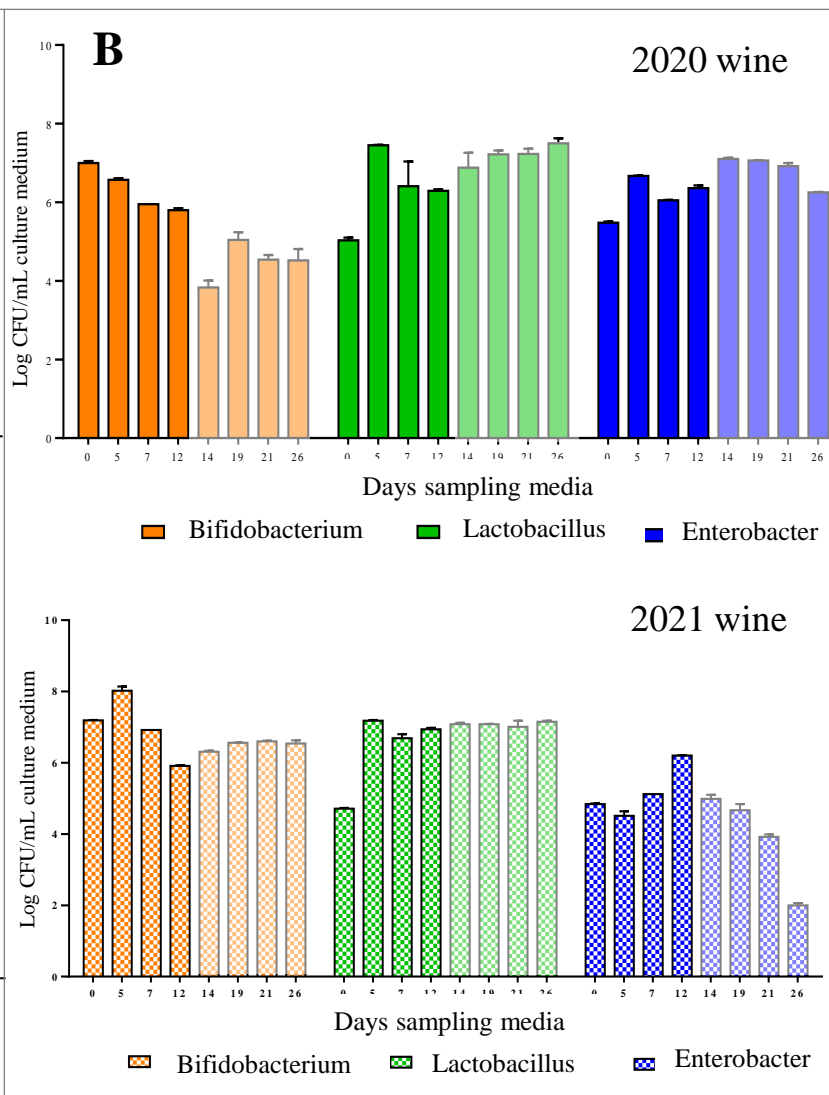
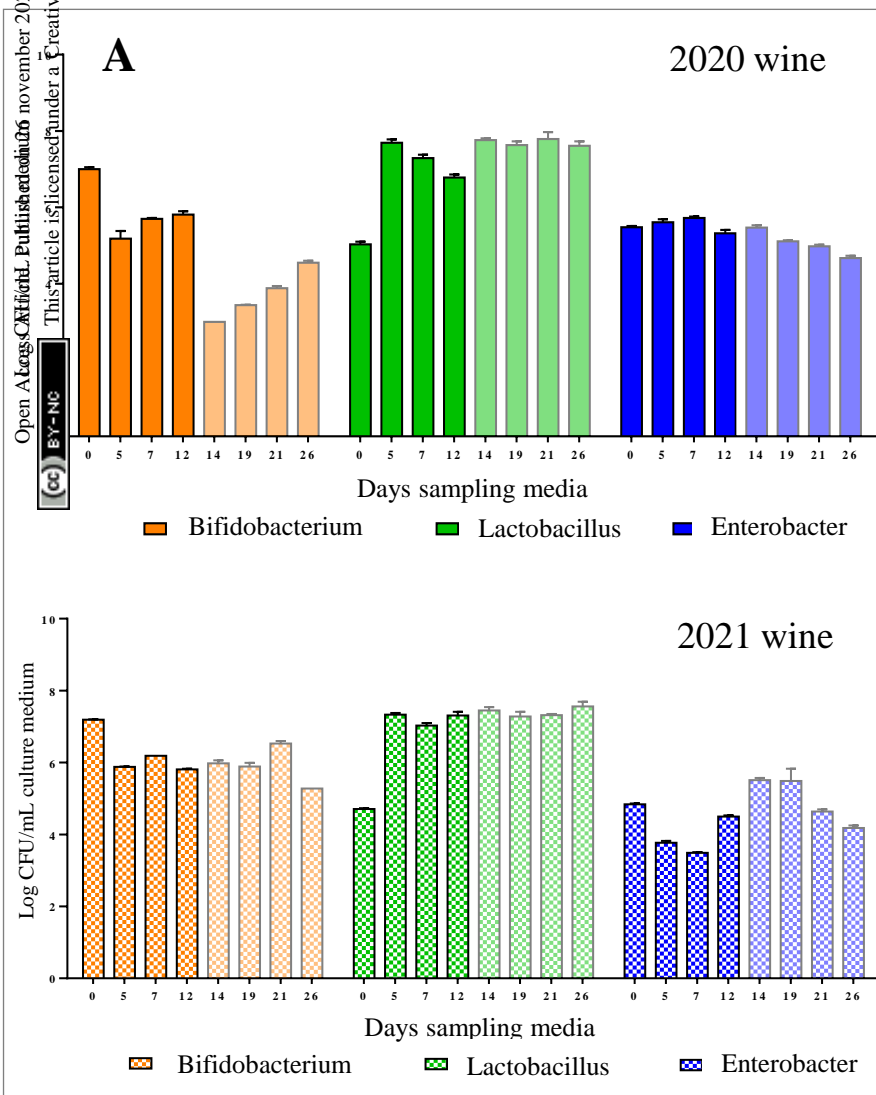
C

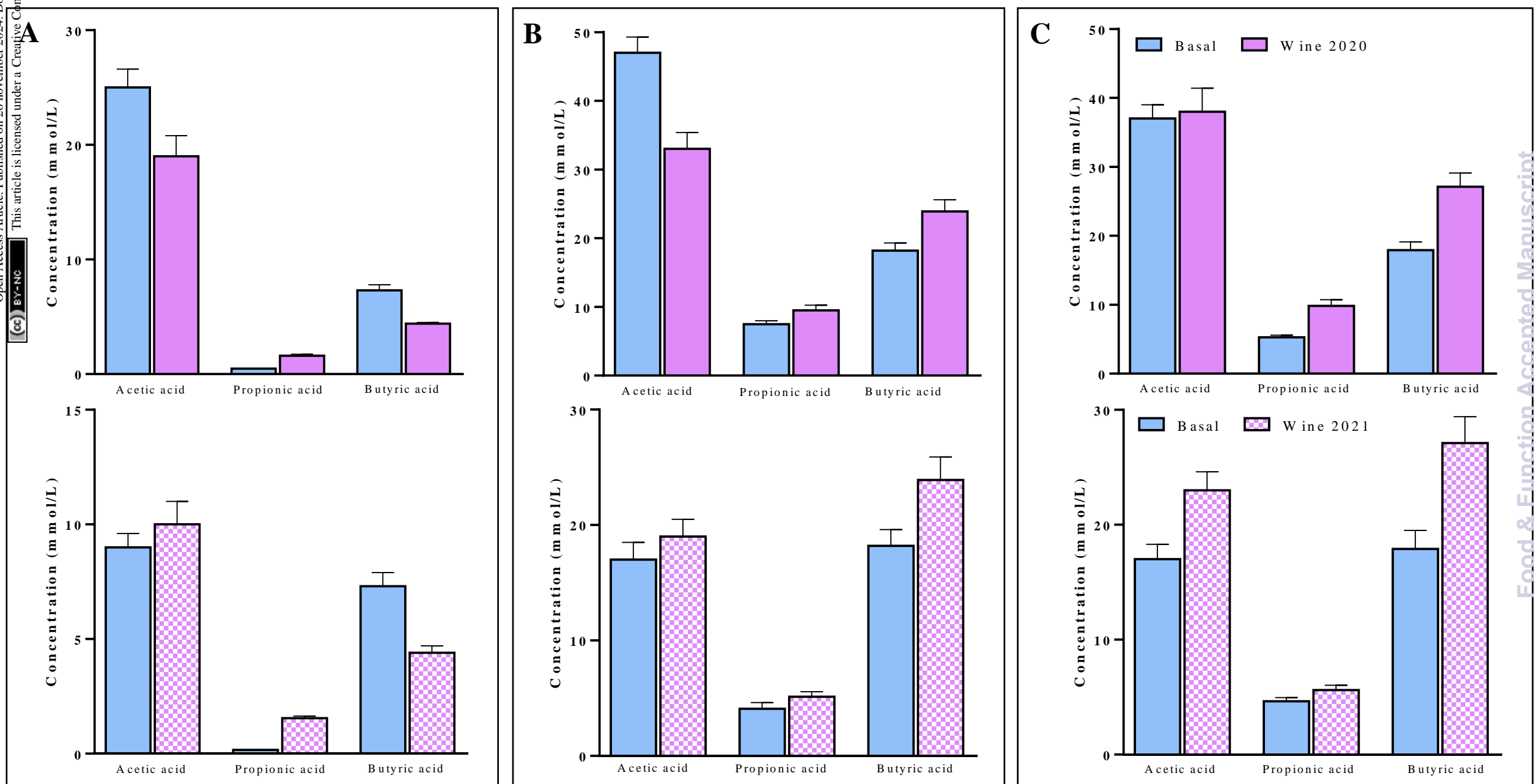


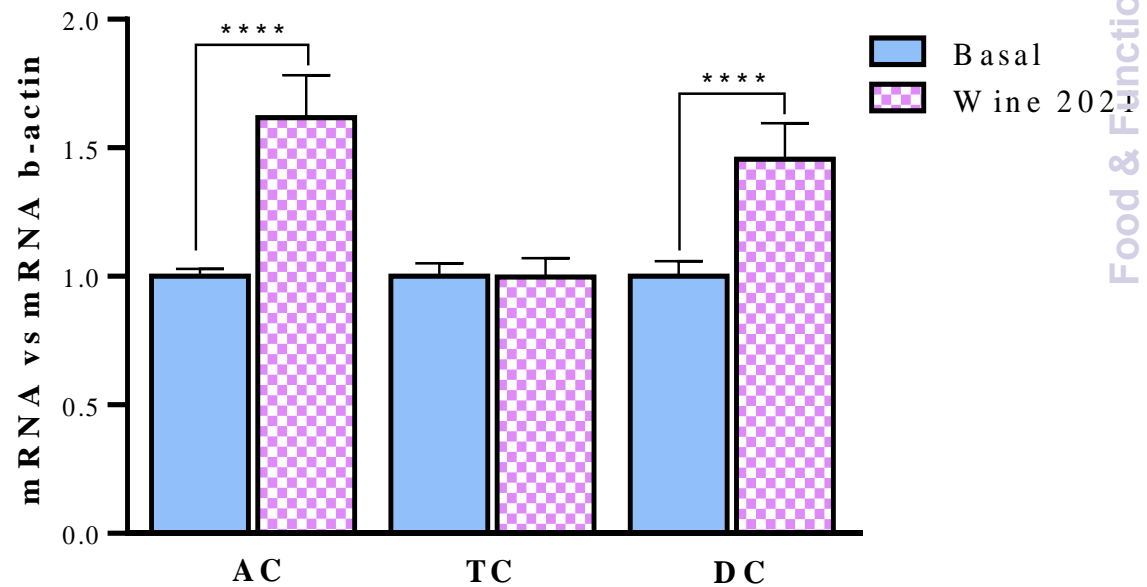
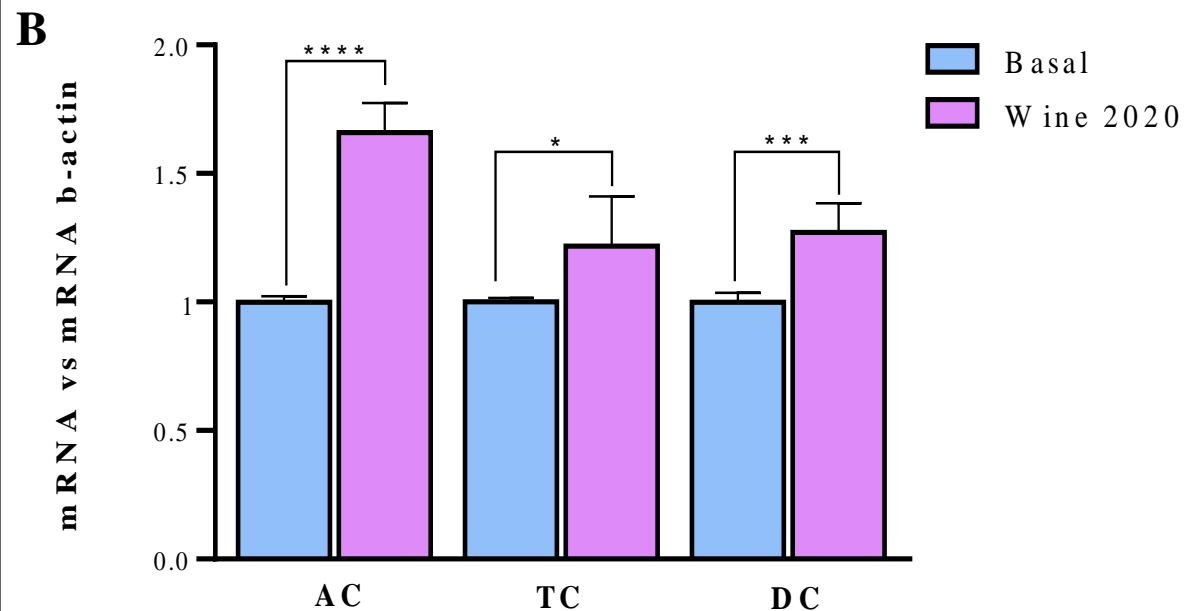
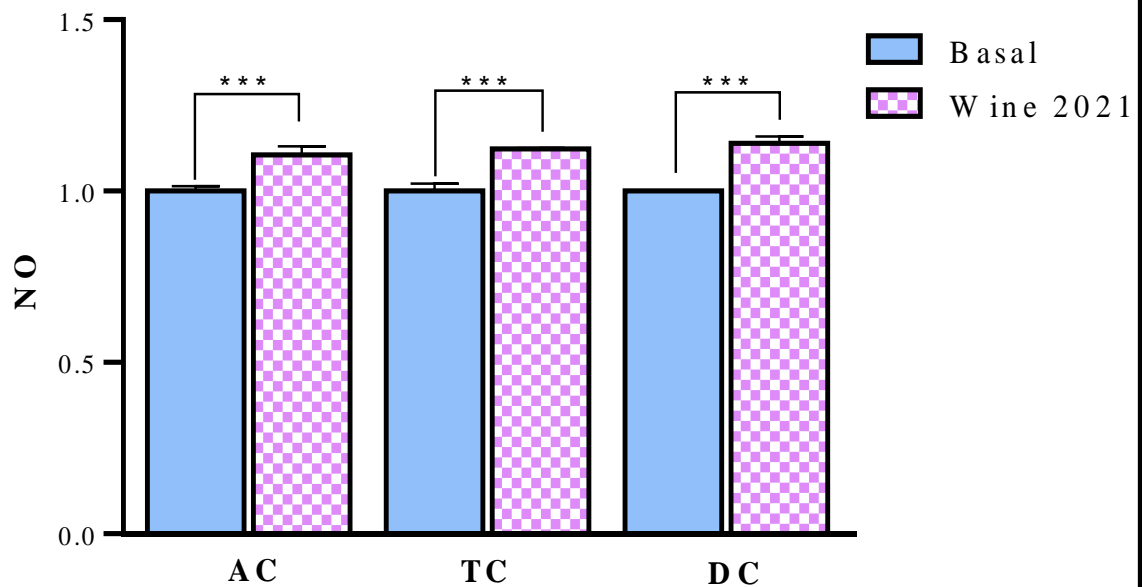
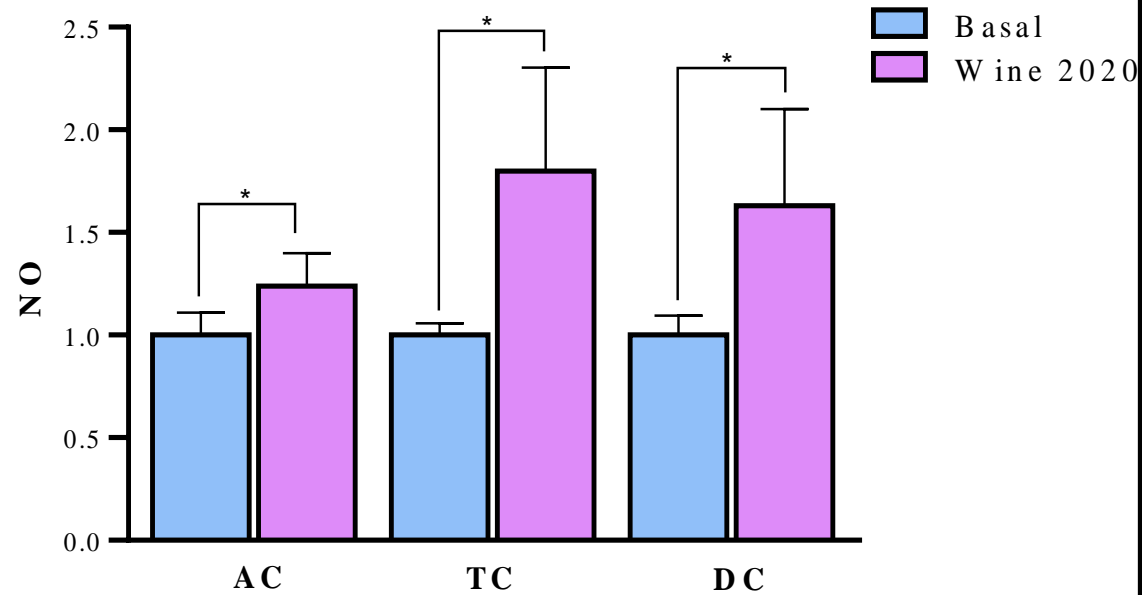
Open Access Article. Published on 26 November 2024. Downloaded on 26/11/2024 01:00:56.
This article is licensed under a Creative Commons Attribution-NonCommercial 3.0 Unported Licence.

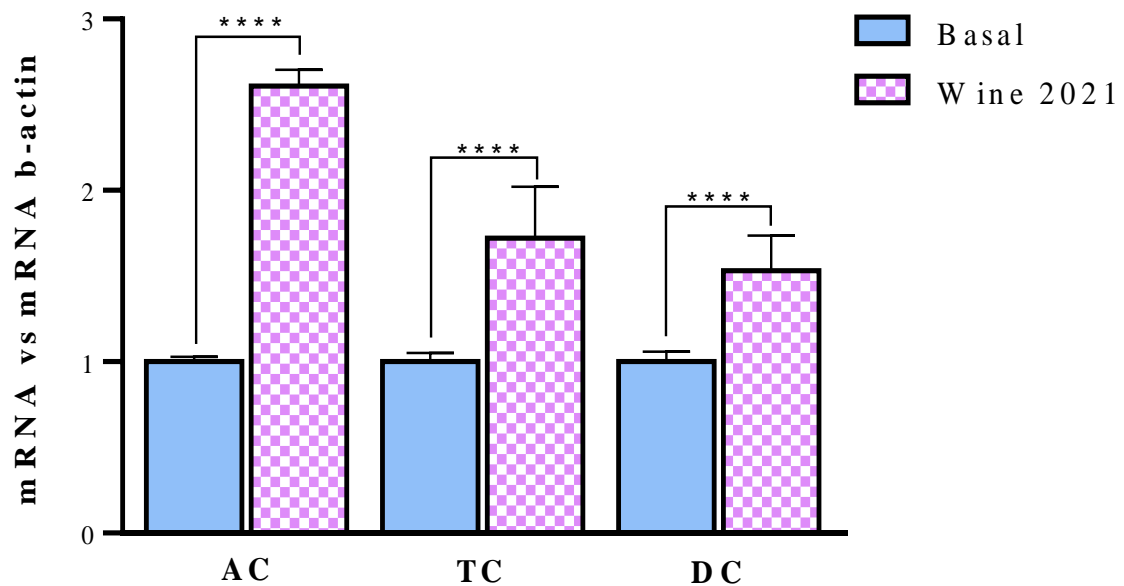
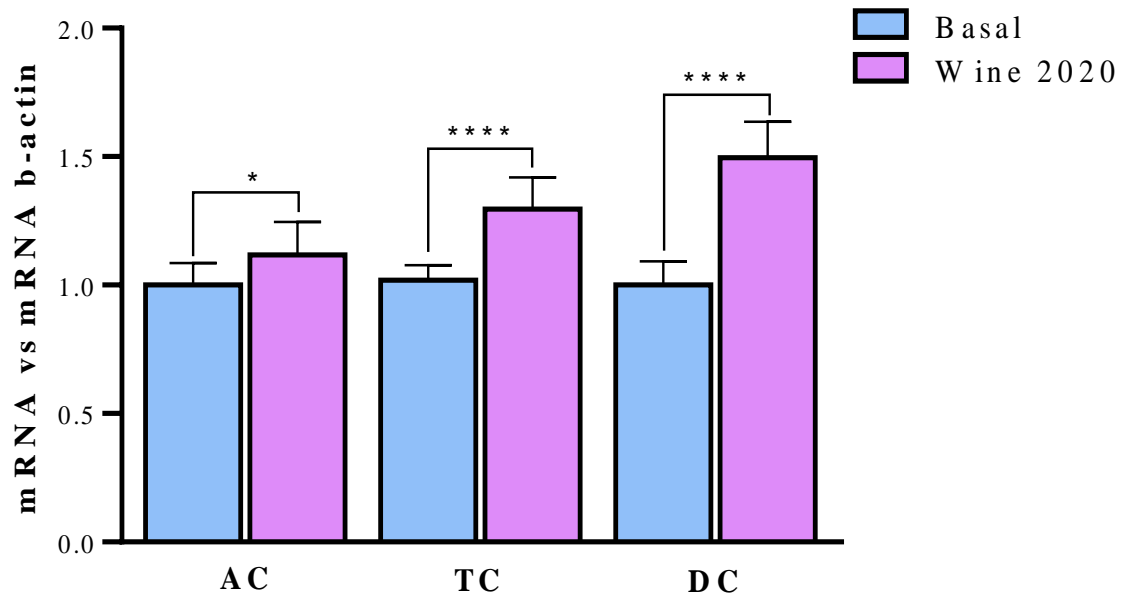


Food & Function Accepted Manuscript









B

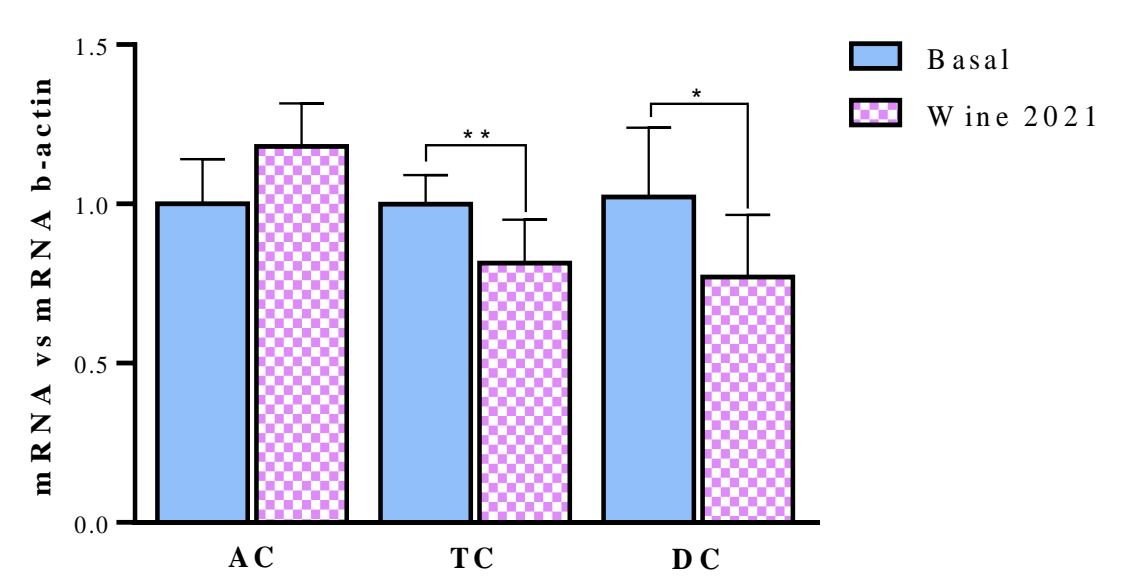
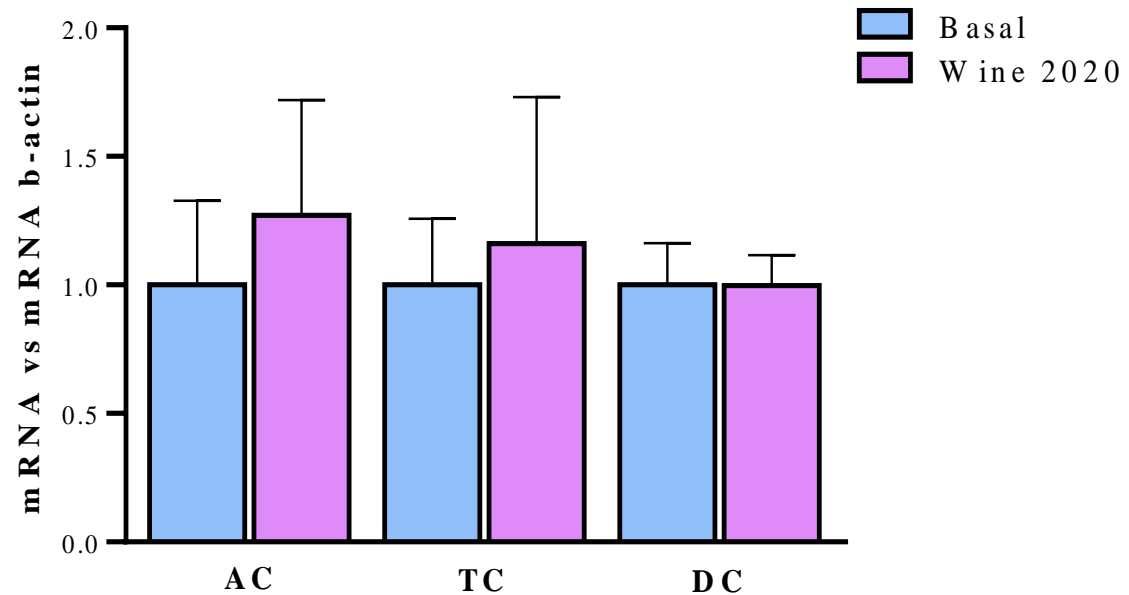


Figure 8

